iScience

CellPress
OPEN ACCESS

Article

SIRT2 inhibition by AGK2 enhances mycobacteria-specific stem cell memory responses by modulating beta-catenin and glycolysis

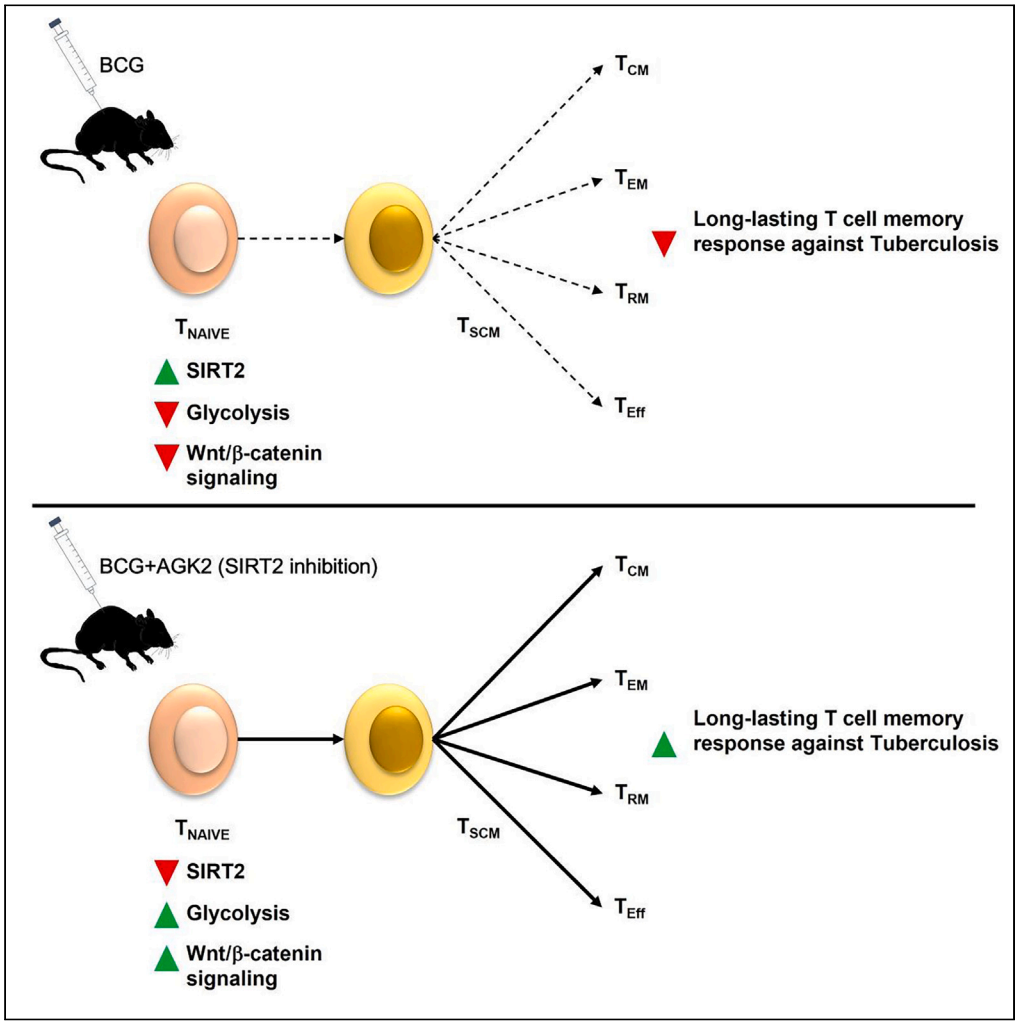

Ashima Bhaskar, Isha Pahuja, Kriti Negi, ..., Jaswinder Singh Maras, Shivam Chaturvedi, Ved Prakash Dwivedi

ashimabhaskar@gmail.com

Highlights

SIRT2, a class III HDAC, is overexpressed in *M.tb*-specific $CD4^+$ T cells

SIRT2 inhibition enhances β-catenin acetylation and glycolysis in $CD4^+$ T cells

SIRT2 inhibition strengthens the stem cell memory phenotype of $CD4^+$ T cells

SIRT2 inhibition enhances the vaccine efficacy of BCG

Bhaskar et al., iScience *26*, 106644
May 19, 2023
https://doi.org/10.1016/j.isci.2023.106644

iScience

CellPress
OPEN ACCESS

Article

SIRT2 inhibition by AGK2 enhances mycobacteria-specific stem cell memory responses by modulating beta-catenin and glycolysis

Ashima Bhaskar,[1,4,*] Isha Pahuja,[1,2] Kriti Negi,[1] Akanksha Verma,[1] Antara Ghoshal,[1] Babu Mathew,[3] Gaurav Tripathi,[3] Jaswinder Singh Maras,[3] Shivam Chaturvedi,[1] and Ved Prakash Dwivedi[1]

SUMMARY

Bacille Calmette-Guerin (BCG) generates limited long-lasting adaptive memory responses leading to short-lived protection against adult pulmonary tuberculosis (TB). Here, we show that host sirtuin 2 (SIRT2) inhibition by AGK2 significantly enhances the BCG vaccine efficacy during primary infection and TB recurrence through enhanced stem cell memory (T_{SCM}) responses. SIRT2 inhibition modulated the proteome landscape of $CD4^+$ T cells affecting pathways involved in cellular metabolism and T-cell differentiation. Precisely, AGK2 treatment enriched the IFNγ-producing T_{SCM} cells by activating β-catenin and glycolysis. Furthermore, SIRT2 specifically targeted histone H3 and NF-κB p65 to induce proinflammatory responses. Finally, inhibition of the Wnt/β-catenin pathway abolished the protective effects of AGK2 treatment during BCG vaccination. Taken together, this study provides a direct link between BCG vaccination, epigenetics, and memory immune responses. We identify SIRT2 as a key regulator of memory T cells during BCG vaccination and project SIRT2 inhibitors as potential immunoprophylaxis against TB.

INTRODUCTION

Tuberculosis (TB) is an infectious disease caused by the intracellular pathogen *Mycobacterium tuberculosis* (*M.tb*). It is transmitted via expelled *M.tb*-contaminated aerosols and primarily attacks the lungs of infected individuals. Subsequently, to obstruct infection, the host elicits a foray of antimycobacterial defense mechanisms by activating the innate and adaptive immune responses.[1] *M.tb* on the other hand has complex mechanisms to modulate these defences and circumvent host immune mechanisms.[2] Despite accessibility to standard anti-TB treatment (ATT), 1.4 million individuals died and 10 million people were infected with TB in 2019.[3] Moreover, prophylactic immunization with a live attenuated strain of *Mycobacterium bovis*, Bacille Calmette-Guerin (BCG), fails to control the massive incidence of TB cases annually, indicating the need for an efficacious complementary TB control strategy.

BCG was developed 100 years ago with piecemeal knowledge of fundamental immune determinants with the aim to protect neonates from *M.tb* infection. Eventually, the vaccination strategy was extended for pulmonary TB. Although BCG is known to protect against disseminated forms of TB in children, this protective immunity gradually disappears, and as a result, it is mostly inadequate against adult pulmonary TB and cannot inhibit primary infection or recrudescence of latent TB.[4] BCG has been shown to epigenetically reprogram and augment effector functions of the innate immune cells; however, the conferred protection is merely for a short period and wanes out in adults.[5,6] The incompetence of BCG to aptly stimulate polarization of T-helper cells impedes the expansion of *M.tb*-specific subsets of memory T cells.[7] The inability of BCG to generate adequate adaptive memory responses reflects its poor efficacy in protecting against adult pulmonary TB. Reinforcement of central memory T cells (T_{CM}) to effector memory T cells (T_{EM}) ratio is requisite for lasting protection against TB.[8] Moreover, expansion of the long-lasting, self-restorative T stem cell memory cell (T_{SCM}) population is vital, as they can proficiently differentiate into a spectrum of effector T subsets.[9]

BCG generates trained innate immune cells by inducing epigenetic reprogramming and provides cross-protection against various disease conditions.[10] Therefore, enormous efforts are underway to improve

[1]Immunobiology Group, International Centre for Genetic Engineering and Biotechnology, Aruna Asaf Ali Marg, New Delhi 110067, India

[2]Department of Molecular Medicine, Jamia Hamdard University, New Delhi, India

[3]Department of Molecular and Cellular Medicine, Institute of Liver and Biliary Sciences, New Delhi, India

[4]Lead contact

*Correspondence: ashimabhaskar@gmail.com

https://doi.org/10.1016/j.isci.2023.106644

the efficacy of BCG by targeting innate immune responses.[11] However, no study explores a direct link between BCG vaccination, epigenetics, and host adaptive memory immune responses.

Being actively involved in varied aspects of T-cell development, activation, and differentiation, the role of histone deacetylases (HDACs) in adaptive memory generation during BCG vaccination remains unexplored.[12,13] Lately, sirtuins, NAD^+-dependent class III HDACs, have emerged as crucial regulators of T-cell-mediated adaptive immune responses.[14] Among the seven sirtuins present in mammals, sirtuin 2 (SIRT2) is a cytosolic HDAC known to shuttle to the nucleus during mitosis[15] and certain bacterial infections.[16,17] With a considerable role in critical cellular processes such as metabolism, energy homeostasis, tumor suppression, and inflammation,[18] limited studies demonstrate the role of SIRT2 in T-cell memory responses.[19]

Recently, we reported significant upregulation of SIRT2 in the $CD4^+$ T cells derived from the lungs of *M.tb*-infected mice as compared to the naive mice. In this study, we performed the whole proteome analysis of BCG-primed $CD4^+$ T cells treated with AGK2, which is a specific SIRT2 inhibitor.[20] AGK2 treatment exerted a positive impact on the global proteome landscape of $CD4^+$ T cells where it specifically induced proteins involved in T-cell activation, inflammation, metabolism, and Wnt signaling. In response to oxidative stress, SIRT2 obstructs Wnt signaling by directly interacting and binding to β-catenin.[21] Moreover, SIRT2 is known to inhibit glycolysis and oxidative phosphorylation in murine T cells.[19] Wnt-β-catenin signaling promotes the expansion of self-restorative, long-lived T_{SCM} with proliferative and multipotent abilities to differentiate into an entire range of effector T cells.[19] Furthermore, memory T cells primarily depend on oxidative phosphorylation and glycolysis for energy,[22] and modulating energy metabolism has been shown to assist the formation and maintenance of $CD8^+$ memory T cells.[23,24] Therefore, we hypothesized that the chemical inhibition of SIRT2 during BCG vaccination might increase the generation and maintenance of the T_{SCM} population to enrich the T-cell-mediated adaptive memory responses.

Indeed, the inhibition of SIRT2 in the lymphocytes derived from BCG-vaccinated mice heightened the percentage of interferon gamma (IFNγ)-producing T_{SCM} population. SIRT2 was highly expressed in the $CD4^+$ T_{SCM} cells where it deacetylated histone H3 and nuclear factor kappa B (NF-κB) p65 to modulate the proinflammatory cytokine responses. Furthermore, the impact of SIRT2 inhibition on β-catenin acetylation and glycolysis led to the increased production of stem cell memory responses. As a result, AGK2 treatment in adjunct with BCG immunization considerably augmented the effectiveness of BCG in response to primary infection, reinfection, and recrudescence in mice. Adoptive transfer experiments in *Rag1*$^{-/-}$ mice confirmed that the adaptive immune responses generated during BCG-AGK2 coimmunization were *M.tb*-specific. Lastly, simultaneous inhibition of SIRT2 and β-catenin *in vivo* abrogated the generation of T-cell-mediated adaptive memory responses, thus decreasing the BCG vaccine efficacy. Collectively, the data infer that SIRT2 is a key regulator of memory T cells during TB pathogenesis and indicates the potential of SIRT2 inhibitors as adjunct prophylactic drugs against TB.

RESULTS

AGK2 treatment induces changes in the global proteome landscape of BCG-primed $CD4^+$ T cells

We have recently shown that *M.tb* utilizes SIRT2 to modulate the host immune responses, and SIRT2 inhibition can result in reduction in bacterial load and pathological damage.[17] Because SIRT2 was highly upregulated in $CD4^+$ T cells isolated from *M.tb*-infected mice,[17] we investigated the influence of SIRT2 inhibition of the proteome profile of $CD4^+$ T cells isolated from the lungs of BCG-vaccinated and *M.tb*-infected mice (Figure 1A). For SIRT2 inhibition, the $CD4^+$ T cells were treated with AGK2, which is a very specific SIRT2 inhibitor with an IC_{50} (half-maximal inhibitory concentration) of 3.5 μM and minimally affects the activity of other sirtuins even at a 10-fold high concentration.[25] AGK2 treatment led to a differential expression of 1631 proteins in the *M.tb*-primed $CD4^+$ T cells (Figure 1B) wherein the expression of 1302 proteins was enhanced after AGK2 treatment while 329 proteins were downregulated (Figure 1B), indicating a positive influence of SIRT2 inhibition on $CD4^+$ T-cell proteome landscape (Table S1). Further pathway analysis of these proteins revealed several pathways that were significantly upregulated (Table S2) and downregulated in the $CD4^+$ T cells upon AGK2 treatment (Table S3). Many pathways involved in cellular metabolism, cytokine responses, and intracellular signaling were upregulated by AGK2 treatment (Figure 1C). Interestingly, the Wnt/β-catenin signaling pathway, which plays a crucial role in maintaining memory T cells,[26] was significantly upregulated upon SIRT2 inhibition (Figure 1C). Many proteins that are known to directly or

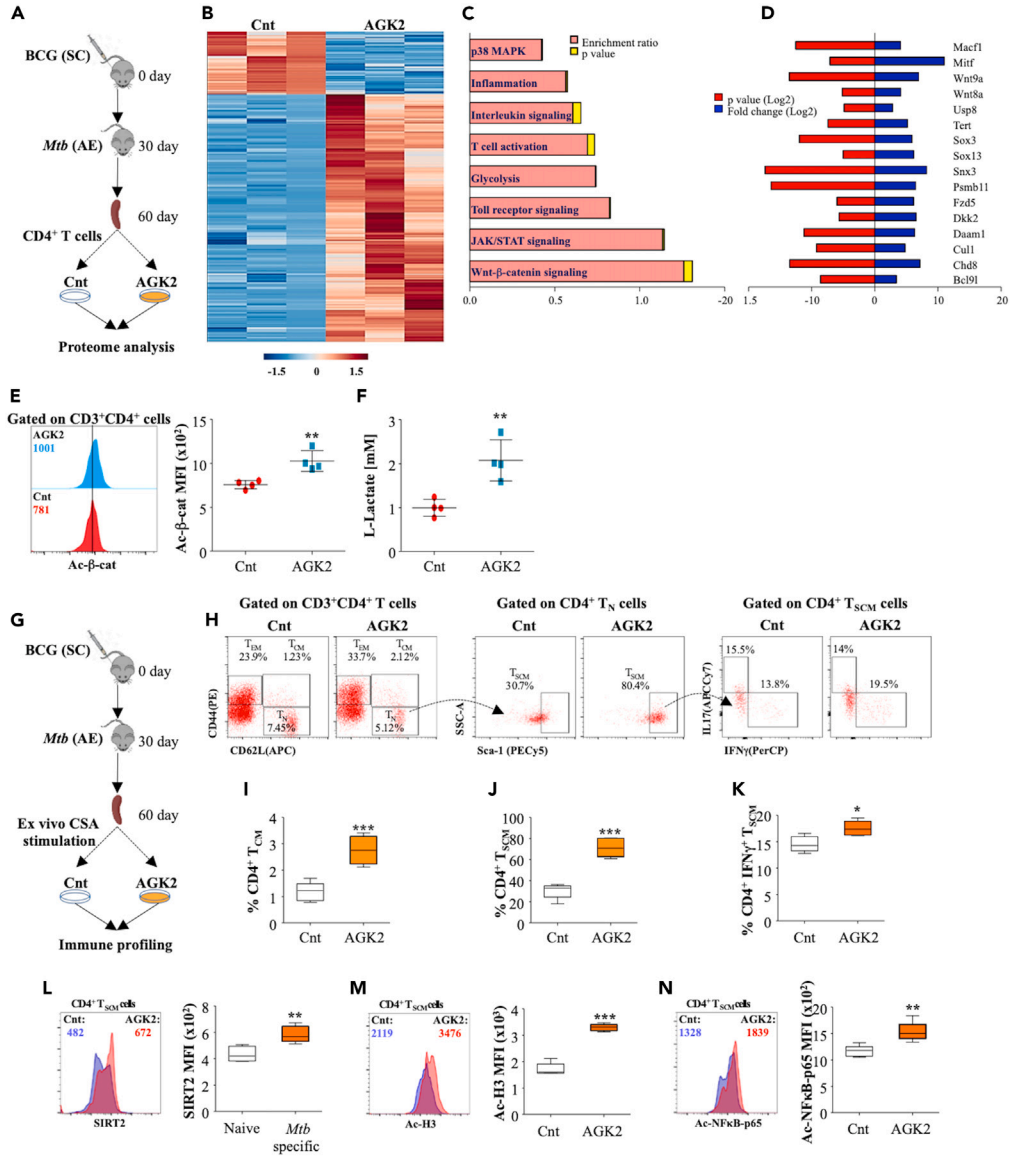

Figure 1. Pharmacological SIRT2 inhibition induces global changes in the proteome landscape of CD4⁺ T cells

(A) $CD4^+$ T cells sorted from the spleen of BCG-vaccinated and *M.tb*-infected mice were *ex vivo* stimulated with *M.tb* complete soluble antigen (CSA) for 48 h followed by treatment with 10-μM AGK2 for 24 h. These cells were subjected to global proteome analysis using mass spectrometry.

(B) Heatmap interpretation of the mass spectrometry proteome profiling of $CD4^+$ T cells (Log2 fold, n = 3). Red represents upregulation while blue depicts downregulation.

(C) Pathways that are significantly upregulated in the AGK2-treated $CD4^+$ T cells.

(D) Wnt/β-catenin pathway proteins upregulated in the AGK2-treated $CD4^+$ T cells.

(E) Representative histograms and the expression of acetylated β-catenin in the $CD4^+$ T cells with or without AGK2 treatment.

(F) Extracellular L-Lactate concentration in the supernatant of $CD4^+$ T-cell cultures with or without AGK2 treatment.

(G) Splenocytes from BCG-vaccinated and *M.tb*-infected mice were *ex vivo* stimulated with *M.tb* CSA for 48 h followed by treatment with 10-μM AGK2 for 24 h. Memory cells were analyzed by staining with anti-CD3 (Pacific Blue), anti-CD4 (PerCPCy5.5), anti-CD8 (APCCy7), anti-CD62L (APC), anti-CD44 (PE), anti-Sca1 (PECy5), anti-IFNγ (BV510), and IL17 (BV650).

(H–K) Representative dot plots and percentage of (I) $CD4^+$ T_{CM} cells, (J) $CD4^+$ T_{SCM} cells, and (K) IFNγ-producing $CD4^+$ T_{SCM} cells in the control and AGK2-treated splenocytes.

Figure 1. *Continued*

(L–N) Representative histograms and the expression of SIRT2 in the naive and *M.tb*-specific $CD4^+$ T_{SCM} cells. Representative histograms and quantification of (M) acetylated histone H3 and (N) acetylated NF-κB p65 levels in the control and AGK2-treated $CD4^+$ T_{SCM} cells. Data are representative of two independent experiments. The graphs represent mean ± SD (n = 4). *p < 0.05, **p < 0.005, ***p < 0.0005.

indirectly activate β-catenin were highly upregulated in $CD4^+$ T cells after AGK2 treatment (Figure 1D), such as Fzd5,[27] Dkk2,[28] Mitf,[29] Macf1,[30] Wnt8a,[31] and Wnt9a.[27]

Activation of Wnt/β-catenin signaling is often linked with enhanced generation of memory stem T cells[32] while SIRT2 is known to inhibit this pathway by deacetylating β-catenin[21] and by modulating the GSK3β functions.[33] We observed a significant increase in the acetylated β-catenin levels in the *M.tb*-primed $CD4^+$ T cells upon AGK2 treatment (Figure 1E). Moreover, SIRT2 inhibited glycolysis in these cells, which may lead to a decrease in the effector functions such as cytokine production[19,34] (Figure 1F). We next investigated if SIRT2 modulates the formation and expansion of memory T cells. For this, *ex vivo* stimulated splenocytes isolated from BCG-vaccinated and *M.tb*-infected mice were treated with AGK2 followed by profiling of different memory T cells (Figure 1G). SIRT2 inhibition led to a significant increase in the percentage of $CD4^+$ T_{CM} cells and T_{EM} cells with a concomitant decrease in T_N cells (Figures 1H and 1I). Among the various memory T cells, T_{SCM} cells possess maximum self-renewal capacity and multipotency and are known to give rise to a spectrum of effector and memory T-cell subsets.[35] AGK2 treatment also increased the percentage of $CD4^+$ T_{SCM} cells by inducing Sca-1 expression in T_N cells (Figures 1H–1J). Further analysis revealed enhanced IFNγ expression in the $CD4^+$ T_{SCM} cells, indicating T_H1-type host protective phenotype (Figures 1H–1K).

To gain further insight into the role of SIRT2 in the maintenance of memory T cells, we checked the expression SIRT2 in the $CD4^+$ T_{SCM} cells derived from naive and *M.tb*-infected mice. Not only was SIRT2 highly expressed in the $CD4^+$ T_{SCM} cells isolated from *M.tb*-infected mice (Figure 1L), its inhibition led to a significant increase in the acetylated levels of histone H3 (Figure 1M) and NF-κB p65 (Figure 1N), both of which are known to influence the changes in host gene expression and may lead to increased secretion of proinflammatory cytokines such as IFNγ.[36]

AGK2 regulates T-cell memory responses by inhibiting β-catenin and glycolysis

To better understand whether SIRT2 inhibition via AGK2 modulates Wnt/β-catenin signaling and cellular metabolism to shape the T-cell-mediated adaptive memory responses (Figure 2A), the *ex vivo* stimulated splenocytes isolated from BCG-vaccinated and *M.tb*-infected mice were treated with AGK2 in the presence of cardamonin (Card), which is known to promote β-catenin degradation,[37] and 2-deoxy-D-glucose (2DG), which inhibits glycolysis[38] followed by memory cell profiling (Figure 2B). 2DG Significantly affected the ability of AGK2 to reduce T_N cells (Figure 2C) and to increase T_{CM} (Figure 2D) and T_{EM} cells (Figure 2E) while Card cotreatment abolished the increase in $CD4^+$ T_{CM} cells upon AGK2 treatment (Figure 2D). Furthermore, both Card and 2DG treatments significantly decreased the AGK2-induced expression of Sca-1 and CD122 on $CD4^+$ T_N cells, indicating a reduced T_{SCM} response (Figures 2F–2I). IFNγ production by $CD4^+$ T_{SCM} cells was also diminished significantly in 2DG- and AGK2-treated splenocytes (Figures 2J and 2K) which displayed decreased glycolysis compared with AGK2-treated $CD4^+$ T cells (Figure 2L). Overall, these results identify SIRT2-β-catenin axis and SIRT2-mediated energy metabolism as regulators of memory T-cell generation during TB.

BCG vaccination with simultaneous SIRT2 inhibition provides superior resistance against TB

One of the main reasons for its limited efficacy is the failure of BCG to generate a sustained long-lived protective immunity. We and others have shown that epigenetic modulations in the host immune cells can result in enhanced protective responses against TB.[39] For example, SIRT2 inhibition by AGK2 greatly increases the host resistance against *M.tb* by increased macrophage activation and Th1/Th17 differentiation. Furthermore, as AGK2 treatment induced significant generation of T_{SCM} and T_{CM} cells, we explored the prophylactic properties of AGK2 in the BCG vaccination model of TB. We performed an initial experiment with 4 groups of mice—control (Cnt), AGK2, BCG, and BCG + AGK2—and analyzed the bacterial burden 30 days after infection (Figure S1A). BCG + AGK2-vaccinated mice displayed lower bacterial burden in the lungs than the BCG-vaccinated mice (Figure S1B). However, the bacterial load in AGK2-vaccinated mice was similar to that in the Cnt group (Figures S1B andS1C). It was in line with our previous data (PMID: 32697192) where we have shown that Mycobacterial infection induces the expression of SIRT2 in host

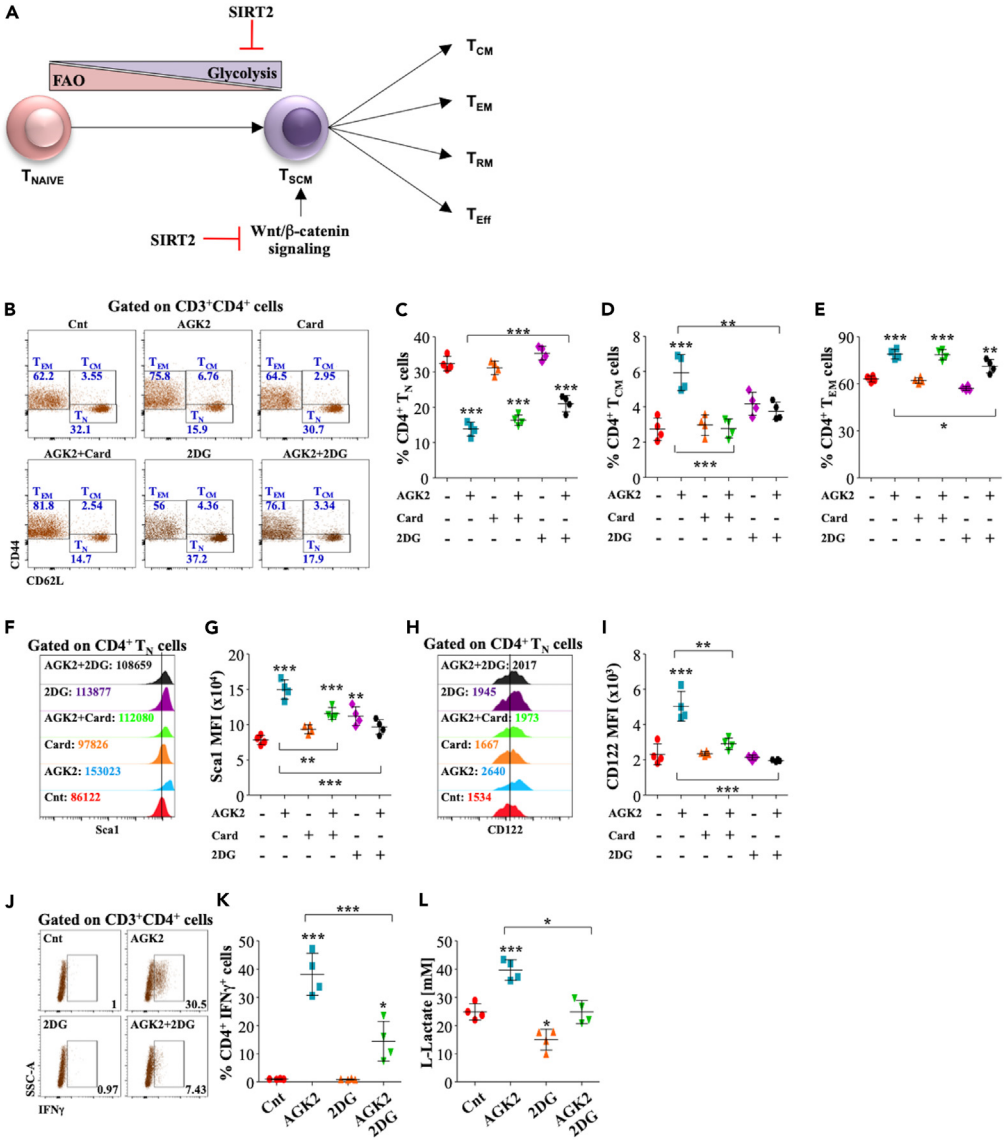

Figure 2. Pharmacological SIRT2 inhibition aids in the generation of memory stem T cells by promoting Wnt/β-catenin signaling and glycolysis

(A) Schematic representation of T-cell differentiation into various memory subsets.

(B-I) *Ex vivo*-stimulated splenocytes were either left untreated or treated with AGK2 (10 μM), Cardamonin (Card; 2.5 μM), and 2-deoxy-D-glucose (2DG; 200 mM) for 24 h. Different memory T cells were analyzed by staining with anti-CD3, anti-CD4, anti-CD62L, anti-CD44, anti-Sca1, and CD122 followed by flow cytometry. (B) Representative dot plots and the percentage of (C) $CD4^+$ T_N cells, (D) T_{CM} cells, and (E) T_{EM} cells in different conditions. (F) Representative histograms and expression of (G) Sca-1 in $CD4^+$ T_N cells. (H) Representative histograms and expression of (I) CD122 in $CD4^+$ T_N cells. (J) FACS dot plots and (K) the percentage of IFNγ-secreting $CD4^+$ T cells with or without treatment with AGK2 and 2DG. (L) *Ex vivo* stimulated splenocytes isolated from BCG-vaccinated and *M.tb*-infected mice were treated with AGK2 and 2DG for 24 h followed by extracellular L-lactate measurements (see STAR Methods). Data are representative of two independent experiments. The graphs represent mean ± SD (n = 4). *p < 0.05, **p < 0.005, ***p < 0.0005.

macrophages, and hence, it was only in the infected macrophages where SIRT2 inhibition/knockdown has any effect on the innate immune modulation. Furthermore, SIRT2 was highly expressed in the T cells isolated from *M.tb*-infected mice compared with the T cells isolated from naive animals. Therefore, we focused our study on the BCG-AGK2 vaccination regime and explored the mechanisms involved in the higher efficacy of this routine. We assessed the efficacy of the vaccine regime by monitoring three deliverables: (1) disease progression in primary infection, (2) disease outcome during reinfection, and (3) rate of

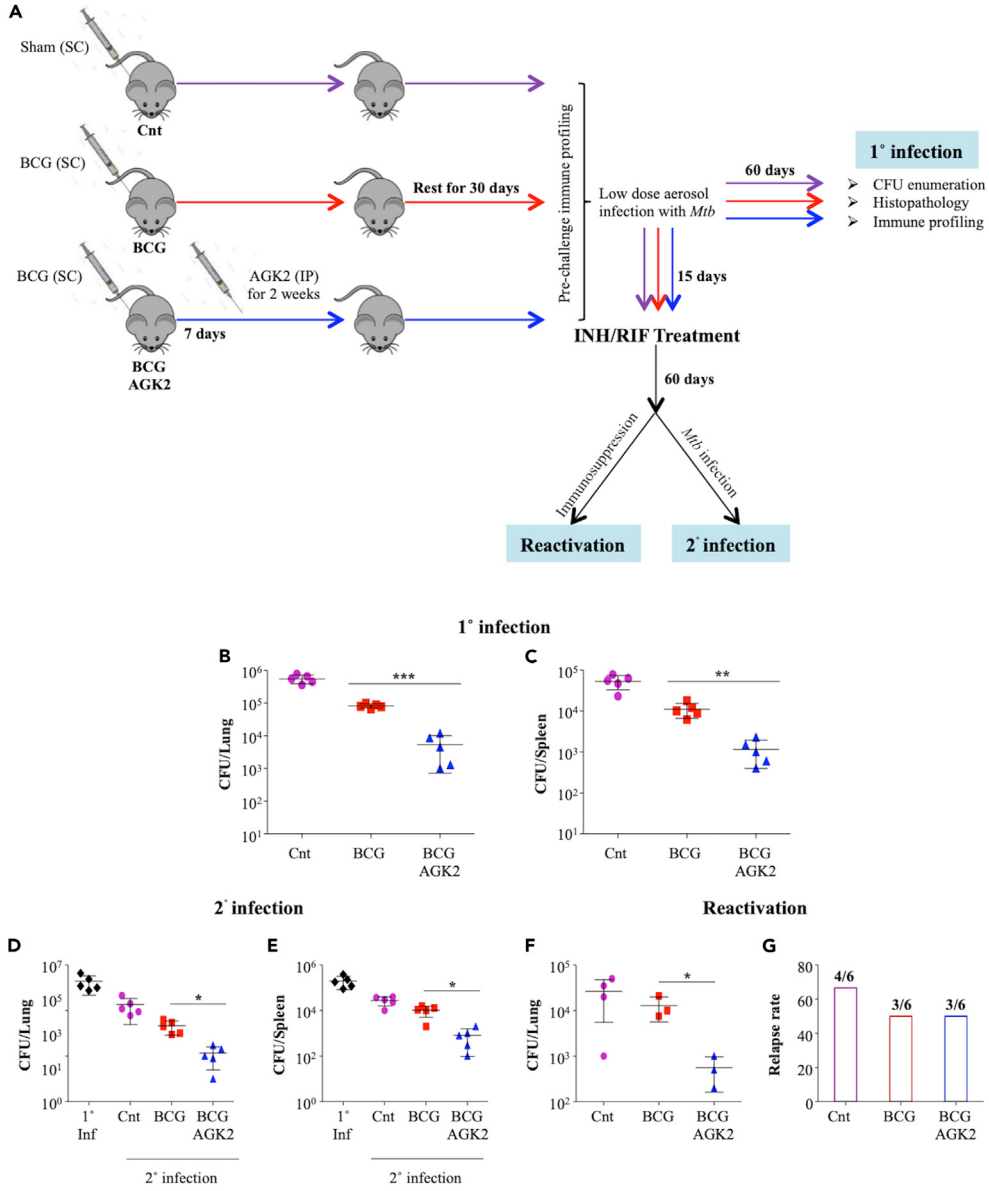

Figure 3. AGK2 enhances the antitubercular efficacy of BCG vaccination

(A–C) Schematic representation of the animal models (primary infection, reinfection, and reactivation) and vaccine regime used for the study. Unvaccinated, BCG-vaccinated, and BCG-vaccinated/AGK2-treated C57/BL6 mice were infected with a low dose of *M.tb* (~100 CFU) and sacrificed 60 days after infection to determine the bacterial burden. CFU in (B) the lungs and (C) the spleen of infected animals.

(D and E) After treatment with isoniazid (INH) and rifampicin (RIF) for 60 days, the mice were reinfected with low-dose *M.tb* followed by CFU determination 30 days after infection. CFU in (D) the lungs and (E) the spleen of reinfected mice.

(F and G) INH/RIF-treated animals were given dexamethasone as an immunosuppressant for 30 days followed by CFU analysis. (F) Bacterial burden in the lungs of relapsed mice. (G) Relapse rate observed in the three groups. Data are representative of two independent experiments with 4–6 mice in each group. The graphs represent mean ± SD.

*p < 0.05, **p < 0.005, ***p < 0.0005.

reactivation (Figure 3A). AGK2 treatment significantly reduced the bacterial burden in the lungs and the spleen of BCG-vaccinated mice during primary infection (Figures 3B and 3C). Owing to severe immune impairment, the current anti-TB therapy, which consists of multiple antibiotics, renders the host vulnerable to reinfections and reactivation, which are associated with higher mortality rates.[40] Interestingly, BCG-AGK2 vaccination displayed enhanced resistance to secondary challenge as evidenced by decreased

bacterial growth in the lungs and the spleen of infected animals (Figures 3D and 3E). Furthermore, immune suppression in isoniazid-/rifampicin-treated mice resulted in significantly lower resuscitation of latent bacilli in terms of bacterial burden (Figure 3F) with a comparable rate of relapse (Figure 3G). Overall, these results demonstrate the remarkable long-term protection conferred by the BCG-AGK2 vaccine strategy.

AGK2 treatment during BCG vaccination activates the innate and adaptive immune cells during TB

Because the host immune system plays a critical role in containing *M.tb*, next, we aimed at understanding the changes in the host immune responses which lead to increased resistance conferred by the BCG-AGK2 combination. First, we analyzed the prechallenge immune status of the unvaccinated and vaccinated mice after 30 days of rest (Figure S2). We observed a significant increase in T-cell activation both in the lungs (Figures S2A and S2B) and the spleen of BCG-AGK2-vaccinated animals (Figures S2C and S2D). Further analysis revealed a Th1/Th17 immune environment in BCG-AGK2-vaccinated mice as evidenced by an increased percentage of IFNγ- and IL17-producing T cells in the lungs (Figures S2E–S2H) and the spleen (Figures S2I–S2L). These data indicate that the BCG-AGK2 combination creates a restrictive environment for mycobacteria in the naive mice, which may contribute to a host of favorable disease outcomes.

During TB, macrophages act as the first line of defense being responsible for phagocytosing the bacilli while dendritic cells process and present bacterial antigens to activate adaptive immunity.[41] Costimulatory molecules such as CD40, CD80, and CD86 present on antigen-presenting cells (APCs) aid in T-cell activation by initiating various cell signaling pathways.[42] Interestingly, 60 days after the *M.tb* challenge, we observed an increased percentage of $CD11b^+$ cells in the lungs of BCG-AGK2 vaccinated (Figures 4A and 4B) which also expressed enhanced levels of costimulatory markers CD40, CD80, and CD86 (Figures 4C–4E). A significant increase in the percentage of $CD11c^+CD40^+$ cells was also observed (Figures 4F–4I). A similar trend was observed in the spleen wherein there was an increased percentage of activated $CD11b^+$ and $CD11c^+$ cells in BCG-AGK2-vaccinated mice (Figures S3A–S3H). Ample evidence indicates an inevitable role of $CD4^+$ and $CD8^+$ T cells in imparting protection against TB.[43,44] Even so, AGK2 treatment did not change the percentage of $CD4^+$ and $CD8^+$ T cells in BCG-vaccinated mice (Figures 4J–4L), and there was an increased expression of early activation marker, CD69, in these mice compared with BCG vaccination alone (Figures 4M and 4N). However, enhanced T-cell activation was not observed in the spleen of BCG-AGK2-vaccinated mice (Figures S3I–S3L).

Polyfunctional T cells secreting more than two cytokines (such as INFγ, IL17, TNFα, and IL2) are considered host protective and may play a role in vaccine-mediated defense.[45] We observed that AGK2 treatment greatly improved the ability of BCG to induce the polyfunctional $CD4^+$ and $CD8^+$ T cells. There was an increased percentage of $CD4^+$ and $CD8^+$ T cells that expressed 4, 3, and 2 cytokines out of INFγ, IL17, TNFα, and IL2 in the lungs (Figures 5A–5D) and the spleen of BCG-AGK2-vaccinated mice (Figures S4A–S4D). Overall, these results indicate that simultaneous AGK2 treatment and BCG vaccination results in the generation of strong host-protective immune responses during TB.

AGK2 treatment strengthens the BCG-induced adaptive memory responses

Several studies indicate the failure of BCG to induce long-lasting memory T-cell responses.[43] Reduced efficacy of BCG in preventing adult pulmonary TB is mainly attributed to the age-related waning of T_{CM} responses.[46] To understand the influence of BCG-SIRT2 inhibition on the induction of adaptive memory *in vivo*, we analyzed the T-cell-mediated adaptive memory responses in the lungs and the spleen of infected animals. SIRT2 inhibition during BCG vaccination significantly improves the percentage of $CD4^+$ and $CD8^+$ T_{CM} cells, with a concomitant decline in the T_{EM} cells resulting in an increase in the T_{CM}/T_{EM} ratio in the lungs of infected animals (Figures 6A–6G). A similar pattern was observed in the spleen of infected animals wherein the T_{CM}/T_{EM} ratio was higher in $CD4^+$ T cells (Figures S5A–S5C). However negligible influence was observed in $CD8^+$ T cells (Figures S5D–S5F). Recent studies stipulate that antigen-specific T_{SCM} cells are the primary source of central memory responses.[47] Interestingly, AGK2 treatment greatly augmented the percentage of T_{SCM} cells in the lungs (Figures 6H–6J) and the spleen of BCG-vaccinated mice (Figures S5G and S5H). Tissue-resident memory T cells (T_{RM}) present in the lungs have been shown to positively regulate the BCG vaccine efficacy.[48] Seldom have we seen instances wherein immune responses are the same in different organs and tissues. TB primarily affects the lungs where T_{RM} population plays a significant role in recall responses during secondary infection. With no difference in the splenic T_{RM} population (Figures S5I and S5J), SIRT2 inhibition greatly enriched the $CD4^+$ and $CD8^+$ T_{RM} population in the lungs of BCG-vaccinated mice (Figures 6K–6M).

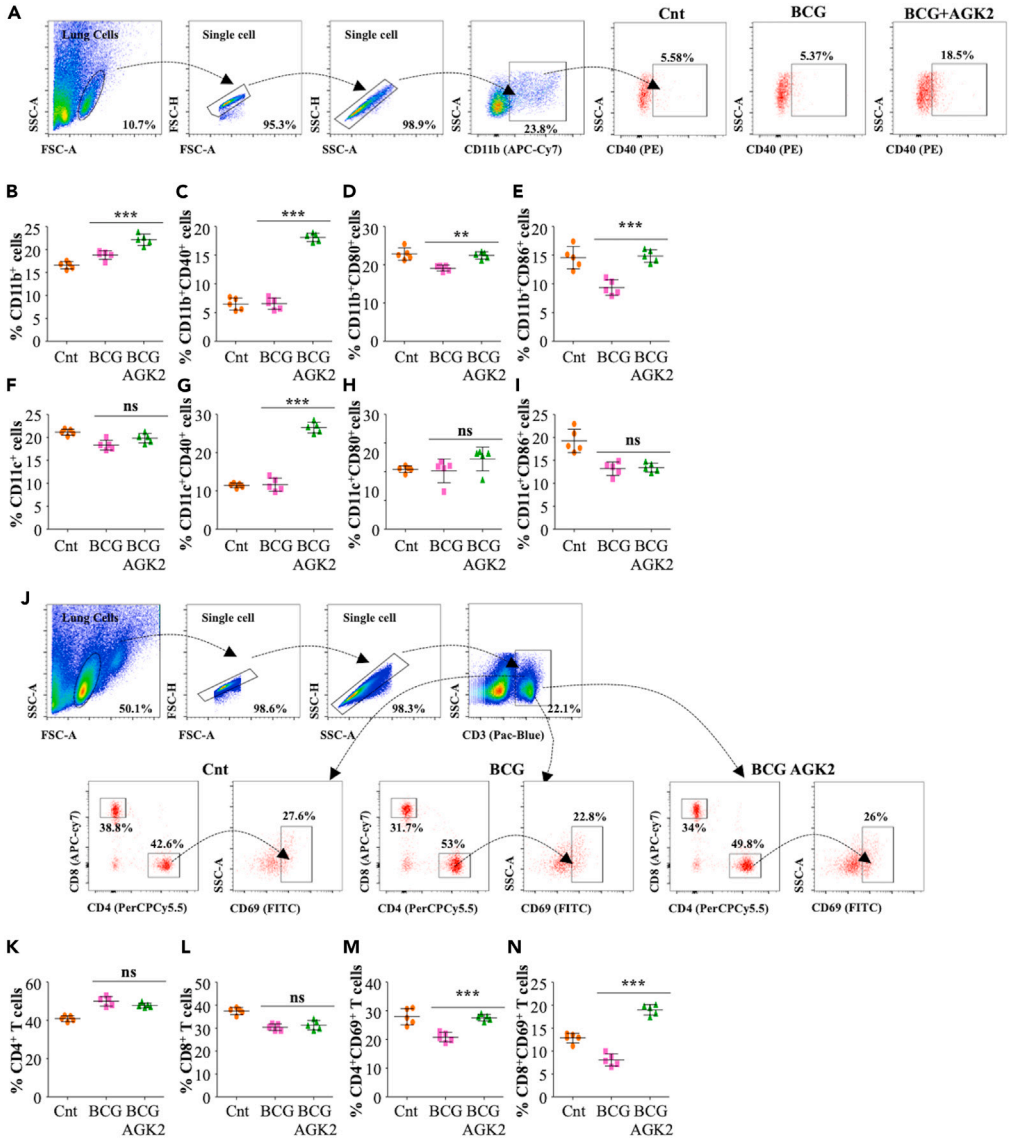

Figure 4. AGK2 enhances the BCG-induced innate and adaptive immune cell activation

(A–I) Gating strategy used to screen the antigen-presenting cells in the lungs and the spleen of infected animals. The cells were *ex vivo* stimulated with *M.tb* CSA for 24 h and stained with anti-CD11b (APCCy7), anti-CD11c (APC), anti-CD40 (PE), anti-CD80 (FITC), anti-CD86 (PerCP). Representative dot plots are shown. Percentage of (B) $CD11b^+$, (C) $CD11b^+CD40^+$, (D) $CD11b^+CD80^+$, and (E) $CD11b^+CD86^+$ in the lungs of infected mice. Percentage of (F) $CD11c^+$, (G) $CD11c^+CD40^+$, (H) $CD11c^+CD80^+$, and (I) $CD11c^+CD86^+$ in the lungs of infected mice.

(J–N) Representative dot plots to demonstrate the gating strategy used. The single-cell suspensions obtained from the lungs of infected animals were stimulated with *M.tb* CSA for 24 h before staining with anti-CD3 (Pacific Blue), anti-CD4 (PreCPCy5.5), anti-CD8 (APCCy7), and anti-CD69 (FITC). Percentage of (K) $CD4^+$, (L) $CD8^+$, (M) $CD4^+CD69^+$, and (N) $CD8^+CD69^+$ T cells. Data are representative of two independent experiments with 5 mice in each group. The graphs represent mean ± SD. *$p < 0.05$, **$p < 0.005$, ***$p < 0.0005$.

Inhibition of β-catenin during BCG vaccination abrogates the AGK2-induced host control of TB

Altogether, the above data strongly suggest that modulation of SIRT2 activity during BCG vaccination results in the generation of superior T-cell memory responses against TB. To further validate whether the higher efficacy of the BCG-AGK2 vaccination regime compared with that of BCG alone is due to enhanced memory responses generated via SIRT2-modulated inhibition of β-catenin, we investigated the influence of

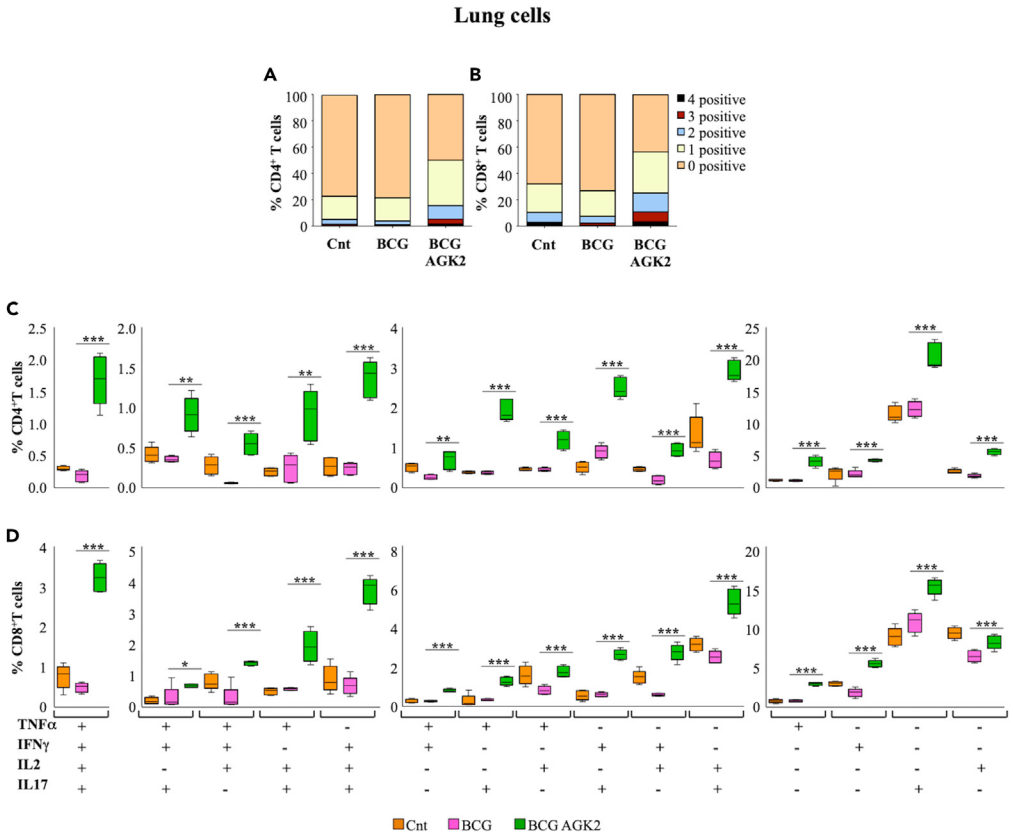

Figure 5. SIRT2 inhibition during BCG vaccination elicits polyfunctional T-cell responses in the lungs of infected mice

(A–D) After *ex vivo* stimulation with *M.tb* CSA, the lung cells were stained with anti-CD3 (Pacific Blue), anti-CD4 (PE), anti-CD8 (APCCy7), anti-IFNγ (APC), anti-IL2 (FITC), and anti-IL17 (PeCy7), and anti-TNFα (PerCP) for polyfunctional cytokine analysis. Proportion of (A) $CD4^+$ and (B) $CD8^+$ T cells positive for 0, 1, 2, 3, and 4 cytokines. Box and whiskers plots depicting the percentage of (C) $CD4^+$ and (D) $CD8^+$ T cells positive for all the possible combinations of the four cytokines examined in the lungs of infected mice. Data are representative of two independent experiments with 5 mice in each group. The graphs represent mean ± SD. *$p < 0.05$, **$p < 0.005$, ***$p < 0.0005$.

β-catenin inhibition on the antitubercular potential of BCG-AGK2 vaccination *in vivo* (Figure 7A). As expected, the prechallenge memory T-cell immune profile indicated the decreased percentage of $CD4^+$ T_N cells in the lungs of BCG-AGK2 mice (Figures 7B and 7C) with a concomitant increase in $CD4^+$ T_{CM} cells while no change was observed in $CD4^+$ T_{EM} cells (Figures 7D and 7E). Card treatment diminished the AGK2-mediated increase in the T_{CM} responses (Figure 7E), further validating that SIRT2 modulates T-cell memory responses via the Wnt/β-catenin pathway. Moderate effects were also seen in the $CD8^+$ memory T cells (Figures S6A–S6C).

To understand the *M.tb*-specific phenotype of these responses, we performed adoptive transfer studies in $Rag1^{-/-}$ mice which lack functional B and T cells.[49] $CD4^+$ T cells isolated from the lungs of vaccinated mice were intravenously injected in naive $Rag1^{-/-}$ mice followed by low-dose aerosol infection with GFP-expressing strain of *M.tb* (Figure 7F). Mice that received $CD4^+$ T cells from BCG-AGK2-vaccinated animals displayed a significant decrease in the lung bacterial load compared with the mice that did not receive any $CD4^+$ T cells or received $CD4^+$ T cells from BCG vaccinated group and BCG-AGK2-Card vaccinated group, indicating a superior killing potential of BCG-AGK2-primed $CD4^+$ T cells (Figure 7G). Consistent with the colony-forming unit data, $CD11b^+MHCII^+$ and $CD11c^+MHCII^+$ APCs in the lungs of BCG-AGK2 $Rag1^{-/-}$ were significantly less infected with Rv-GFP than the other groups (Figures S6D–S6G).

Furthermore, host resistance to *M.tb* infection decreased in BCG-AGK2-Card vaccinated mice compared with BCG-AGK2 vaccination (Figures 7H and 7I) as Card cotreatment decreased the AGK2-mediated

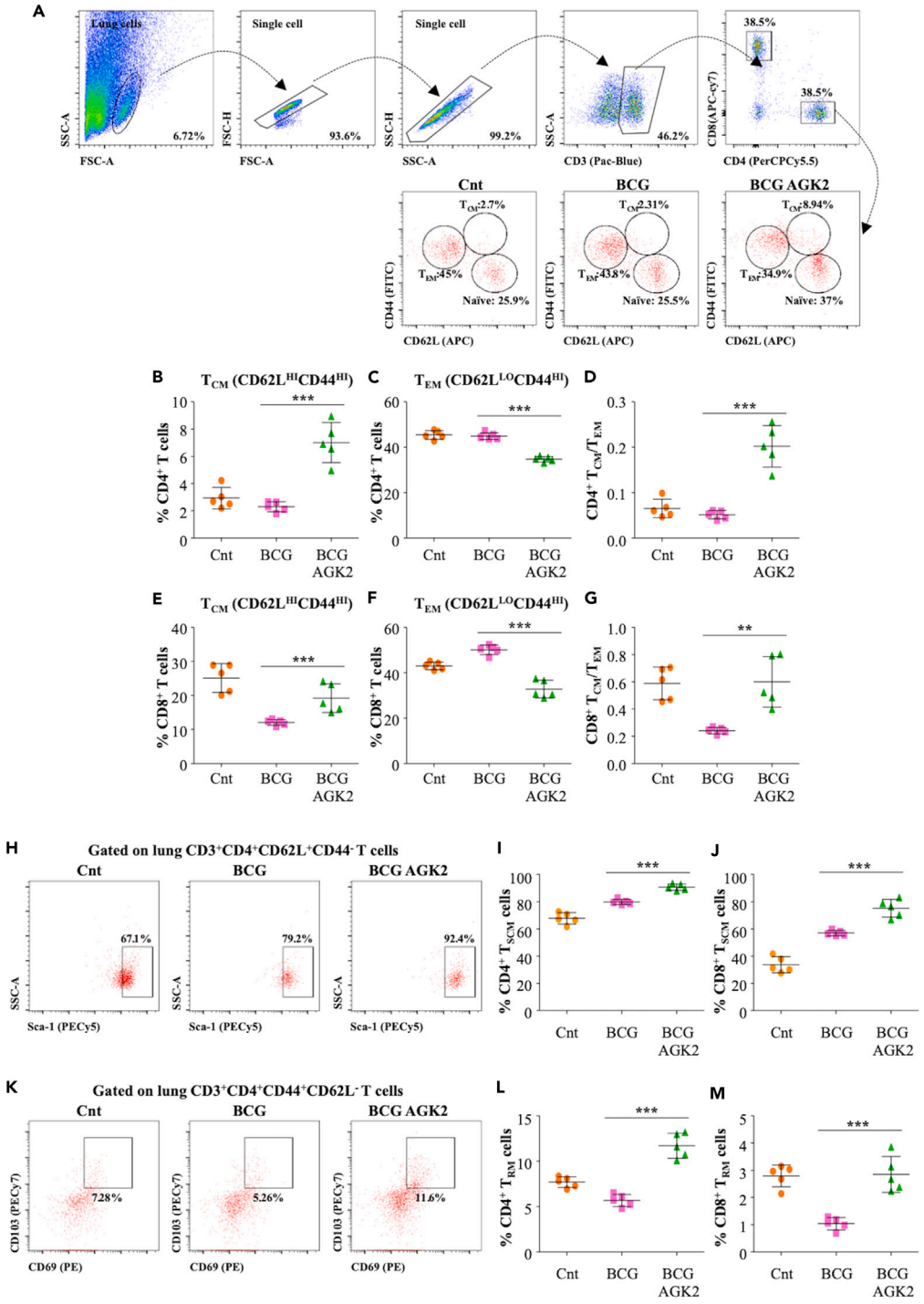

Figure 6. SIRT2 inhibition during BCG vaccination ameliorates memory T-cell responses in the lungs of infected mice

(A–G) Gating technique and representative dot plots for analyzing central memory T-cell responses. *Ex vivo* stimulated single-cell suspensions of infected lungs were stained with anti-CD3 (Pacific Blue), anti-CD4 (PerCPCy.5), anti-CD8 (APCCy7), anti-CD62L (APC), anti-CD44 (FITC), anti-CD69 (PE), anti-CD103 (PEcy7), and anti-Sca1 (PeCy5) for analyzing memory T cells. Percentage of (B) T_{CM} ($CD44^{high}CD62L^{high}$), (C) T_{EM} ($CD44^{high}CD62L^{low}$), and (D) T_{CM}/T_{EM} ratio in the $CD4^+$ T cells present in the lungs of infected mice. Percentage of (E) T_{CM}, (F) $T_{EM,}$ and (G) T_{CM}/T_{EM} ratio in the lung $CD8^+$ T cells.

Figure 6. *Continued*

(H–J) Representative dot plots and quantification of T_{SCM} ($CD44^{-}CD62L^{+}Sca1^{high}$) population in the (I) $CD4^{+}$ and (J) $CD8^{+}$ T cells.

(K–M) Representative dot plots and percentage of T_{RM} ($CD69^{+}CD103^{+}$) population in the (L) $CD4^{+}$ and (M) $CD8^{+}$ T cells. Data are representative of two independent experiments with 5 mice in each group. The graphs represent mean ± SD. *$p < 0.05$, **$p < 0.005$, ***$p < 0.0005$.

activation of $CD4^{+}$ and $CD8^{+}$ T cells (Figures S7A–S7F). Even the central memory and stem cell memory responses were significantly diminished in the lungs of BCG-AGK2-Card mice compared with BCG-AGK2 mice (Figures 7J–7Q) with minimum effect on the T_{EM} and T_N cells (Figures S7G–S7J). Subtle immunological differences were also observed in the spleen of infected animals (Figure S8) wherein Card co-treatment significantly reduced the T-cell activation in the BCG + AGK2-vaccinated animals (Figures S8A–S8D). With hardly any effect on $CD4^{+}$ memory responses (Figures S8E–S8H), Card treatment significantly increased the percentage of $CD8^{+}$ T_N cells, with a concomitant decrease in T_{EM} population (Figures S8I–S8L) further indicating that Card abolishes the ability of AGK2 to drive T_N differentiation into T_{SCM}, $T_{EM,}$ and T_{CM}, which are the major precursors of memory T cells that provide long-term protection against TB.

Overall, the data comprehensively demonstrate that AGK2-mediated protective effects during BCG vaccination could be abolished by inhibiting β-catenin.

DISCUSSION

Vaccination is pivotal for establishing an acquired long-lived state of enhanced defense aimed against combating subsequent infections. Since the introduction of the BCG vaccine as part of the Expanded Program on Immunization by WHO, more than 4 billion individuals have been vaccinated. Despite being the most widely used vaccine of all time, BCG has several shortcomings. Owing to numerous factors, the protective efficacy of BCG is vastly inconsistent, lasts for less than 10–15 years, fails to establish sterilizing immunity against *M.tb* infections, and cannot inhibit primary infection or recrudescence of latent TB. As it is challenging to establish new vaccines, modulation of the host immunity to augment BCG-induced protection can be used as a stratagem to incline immune responses to attain ever-lasting immunity against *M.tb*. Immune responses induced by BCG have been studied comprehensively, and it has been established that BCG epigenetically reprograms innate immune cells and exhibits interim protection.[10] However, BCG-induced epigenetic reprogramming in T cells is a less-travelled area in the field. We have successfully illustrated in our previous study that inhibition of host NAD^{+}-dependent HDAC SIRT2 with chemical inhibitor AGK2 led to significant epigenetic modifications in the innate and the adaptive immune cells generating enhanced host resistance to *M.tb* infection. This further motivated us to evaluate the consequences of SIRT2 inhibition by AGK2 treatment as a prophylactic along with BCG vaccination in the murine model of TB. Since SIRT2 KO mice exhibit significant genomic instability and chromosomal aberration[50] and may not survive during TB because of other comorbidities, we used AGK2 for inhibition of SIRT2 activity with minimal adverse effects on mice.[17] For SIRT2, the IC_{50} of AGK2 is 3.5 μM, whereas it exhibits little activity against SIRT1/3 (IC_{50} > 50 μM). Several studies have used AGK2 as a specific SIRT2 inhibitor to analyze effects of SIRT2 in different disease settings.[25]

Substantial diminution in bacterial load was observed upon AGK2 cotreatment with BCG compared with BCG alone in case of primary *M.tb* infection (Figures 3B and 3C). Attenuation of bacterial load in BCG-AGK2-vaccinated mice became even more evident upon secondary *M.tb* infection (Figures 3D and 3E). Furthermore, the outcomes were consistent in the reactivation model wherein bacterial burden was dramatically lowered upon adjunct AGK2 treatment in relapsed mice (Figure 3F). Altogether, concurrent SIRT2 inhibition resulted in the enhanced antimycobacterial potential of BCG upon *M.tb* infections.

To decipher the contributing factors of enhanced protection during primary and secondary infections, we assessed the impact of BCG-AGK2 prophylaxis on host immune responses. Strengthened T-cell activation was evident in the lungs and spleens of prechallenged BCG-AGK2-vaccinated mice, with the upsurge in IFNγ and IL17 secretion indicating that SIRT2 inhibition augments the host-protective T_H1/T_H17 responses in the BCG-primed mice (Figure S2). These responses were maintained in the lungs of BCG-AGK2-vaccinated mice even 60 days after *M.tb* challenge (Figures 4J–4N).

Components of innate immunity play a vital role in the instigation of host defences upon pathogenic insult. Macrophages and dentritic cells (DCs) function in coherence with cells of adaptive immunity by facilitating

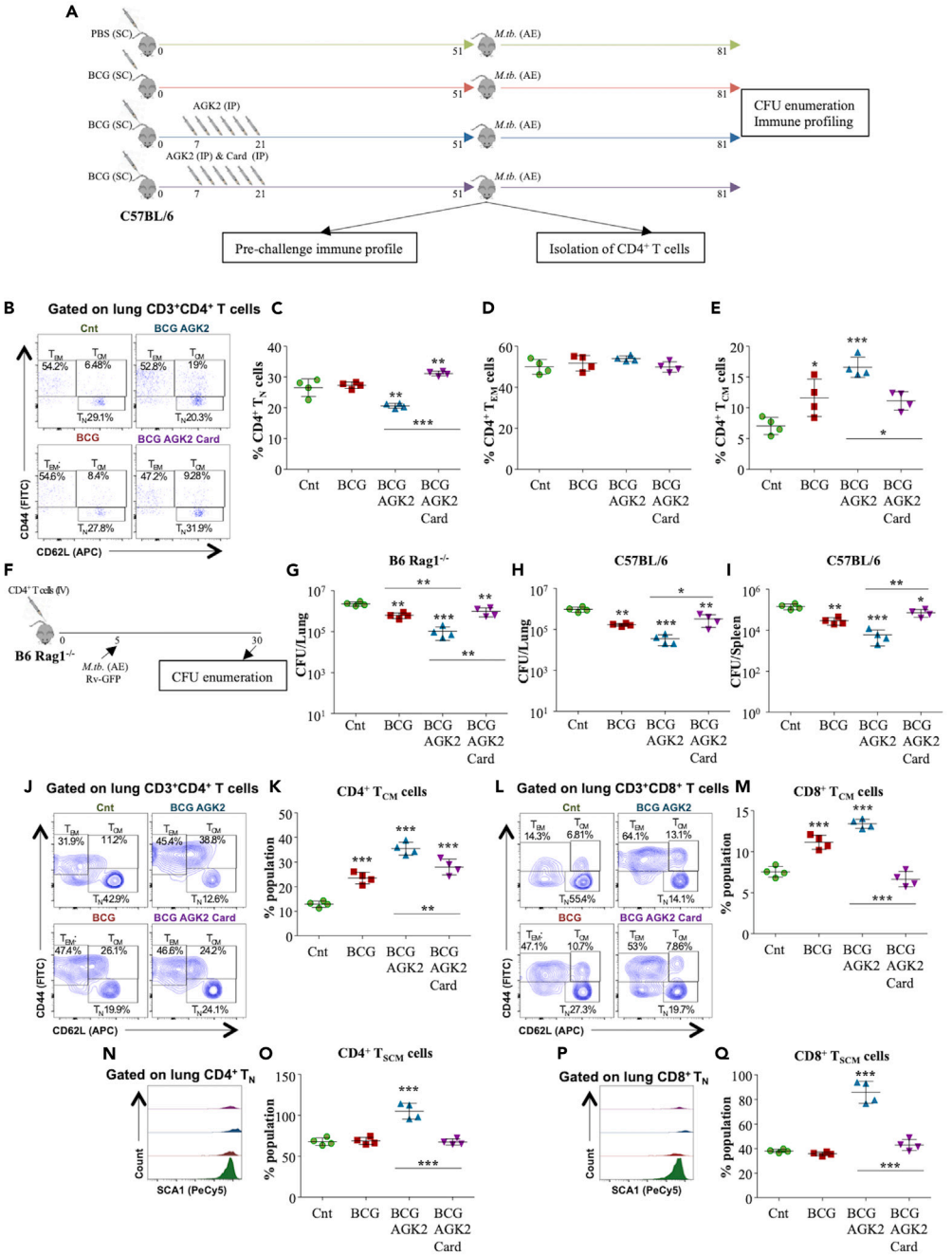

Figure 7. β-Catenin inhibition reverses the AGK2-induced phenotype in the BCG vaccination model of TB

(A) Schematic representation of modified BCG vaccination regime. Seven days after BCG vaccination, mice were either given AGK2 or AGK2 and Card for 2 weeks. After a 30-day rest, mice were sacrificed for analyzing the pre-*M.tb* challenge memory immune responses. The *ex vivo* stimulated lung cells were stained with anti-CD3 (Pacific Blue), anti-CD4 (PerCPCy5.5), anti-CD8 (APCCy7), anti-CD62L (APC), and anti-CD44 (PE) followed by flow cytometry.

(B–E) Representative dot plots and the percentage of (C) $CD4^+$ T_N cells, (D) T_{EM} cells, and € T_{CM} cells in the lungs of vaccinated mice.

(F) $CD4^+$ T cells isolated from the lungs of vaccinated mice were adoptively transferred in naive $Rag1^{-/-}$ mice, which were challenged with Rv-GFP (see STAR Methods).

(G) Bacterial burden in the lungs of $Rag1^{-/-}$ mice 25 days after infection.

(H and I) All the vaccinated animals were challenged with a low dose of *M.tb* (~100 CFU) and sacrificed 30 days after infection to determine the bacterial burden. CFU in (H) the lungs and (I) the spleen of infected animals.

Figure 7. *Continued*

(J-Q) The *ex vivo* stimulated lung cells were stained with anti-CD3 (Pacific Blue), anti-CD4 (PerCPCy5.5), anti-CD8 (APCCy7), anti-CD62L (APC), anti-CD44 (PE), and anti-Sca1 (PECy5) followed by flow cytometry. (J) Representative dot plots and (K) the percentage of $CD4^+$ T_{CM} cells in the lungs of vaccinated mice. (L) Representative dot plots and (M) the percentage of $CD8^+$ T_{CM} cells in the lungs of vaccinated mice. (N) Representative histograms and (O) the expression of Sca1 in the $CD4^+$ T_N cells. (P) Representative histograms and (Q) the expression of Sca1 in the $CD8^+$ T_N cells. Data are representative of two independent experiments. The graphs represent mean ± SD (n = 4). *$p < 0.05$, **$p < 0.005$, ***$p < 0.0005$.

T-cell activation and downstream signaling to bring about proficient defences against *M.tb*. A heightened percentage of $CD11b^+$ and $CD11c^+$ cells collectively with enrichment in costimulatory surface markers ($CD40^+$ and $CD86^+$) was marked in BCG-AGK2-vaccinated and *M.tb*-infected group (Figures 4A–4I). Furthermore, to better comprehend the T-cell responses, we assessed the impact of BCG-AGK2 vaccination on polyfunctional T cells, which can proficiently perform multiple functions by eliciting diverse cytokines.[51] A dramatic rise in the percentage of $CD4^+$ and $CD8^+$ polyfunctional T cells eliciting multiple cytokines such as INFγ, IL17, TNFα, and IL2 was evident in *M.tb*-infected mice vaccinated with BCG-AGK2 (Figure 5). Conclusively it was apparent that inhibition of host SIRT2 enhanced host-protective immune responses stimulated by BCG in response to *M.tb* infection.

Because the shortcomings of the BCG vaccine are compellingly linked with inadequacies in the stimulation of lasting adaptive immune memory, we endeavored to investigate the adaptive memory responses instigated by BCG vaccination along with SIRT2 inhibition. Expansion of $CD4^+$ and $CD8^+$ T_{CM} populations with coexistent regression in the T_{EM} cells was distinctly observed in BCG-AGK2-vaccinated mice. Hence, it was definite that SIRT2 inhibition during BCG vaccination strengthened the T_{CM}/T_{EM} ratio in response to *M.tb* infections (Figures 6A–6G). With the affirmative impact on immunological memory, we further trailed to assess distinctive memory subset, antigen-specific T_{SCM} cells that can generate the entire spectrum of T memory cell populations. SIRT2 inhibition amplified the percentage of $CD4^+$ and $CD8^+$ T_{SCM} cells in the lungs and spleen of BCG-vaccinated mice (Figures 6H–6J). Moreover, T_{RM} confined to major sites of infection were also reinforced dramatically in BCG-AGK2-vaccinated mice (Figures 6K–6M). Hence, we decisively establish the strengthening of T-cell immunological memory responses by inhibiting host SIRT2 coincident with BCG vaccination in the murine model.

We have recently shown that SIRT2 is highly expressed in the *M.tb*-primed $CD4^+$ T cells where it deacetylates histone H3, which may lead to significant changes in the proteome landscape of $CD4^+$ T cells.[17] Satisfactorily, whole proteome analysis revealed a distinct SIRT2-dependent proteome profile in *M.tb*-primed $CD4^+$ T cells (Figure 1B). Further scrutiny unveiled the SIRT2-modulated changes in the Wnt/β-catenin signaling proteins in $CD4^+$ T cells, which play a critical role in the T-cell memory homeostasis[52] (Figure 1D). Other upregulated pathways such as p38 mitogen-activated protein kinase, T-cell activation, Jak/STAT signaling, Toll receptor signaling, interleukin signaling, and inflammation signaling are known to provide host protection against TB.[53,54]

Mechanistic details of $CD8^+$ T_{SCM} generation are well studied, and similar mechanisms are also involved in the generation and expansion of $CD4^+$ T_{SCM} cells.[52] SIRT2 is known to deacetylate β-catenin and temper the functions of GSK3β, resulting in the obstruction of Wnt/β-catenin signaling, which is vital for the generation of stem cell memory,[26] whereas β-catenin is known to directly inhibit SIRT2 expression.[47] Furthermore, it was recently established that SIRT2 inhibition enhanced the effector functions of T cells by promoting glycolysis.[19] Proteome data also suggested upregulation of tricarboxylic acid cycle and glycolysis in AGK2-treated T cells. SIRT2, known to inhibit glycolysis by targeting the glycolytic enzymes,[55] was also shown to modulate the glycolytic activity of resting $CD8^+$ memory T cells in humans.[56] Coherent with this, AGK2 treatment in *M.tb*-primed $CD4^+$ T cells increased the acetylated-β-catenin levels and restrained cells to undergo glycolysis (Figures 1E and 1F). Increased levels of acetylated-β-catenin may promote the accumulation of β-catenin, leading to enhanced expression of β-catenin target genes linked with T-cell memory maintenance.

These intriguing results led us to investigate whether *ex vivo* SIRT2 inhibition resulted in the enhancement of memory responses. To begin with, SIRT2 inhibition resulted in the expansion of $CD4^+$ T_{CM} cells and T_{EM} cells parallel to the reduction in T_N cells (Figure 1H). Similarly, the heightened percentage of $CD4^+$ T_{SCM} cells corresponded with enhanced Sca-1 expression in T_N cells after SIRT2 inhibition (Figure 1J). Moreover, reinforced IFNγ secretion was observed by $CD4^+$ T_{SCM} cells on AGK2 treatment (Figure 1K). Owing to the

prominence of T_{SCM} cells in the formation of memory subsets, the expression of SIRT2 was assessed in the $CD4^+$ T_{SCM} cells. Interestingly, heightened SIRT2 expression was detected in $CD4^+$ T_{SCM} cells with equivalent influence on the known SIRT2 targets, histone H3, and NF-κB p65, which can be correlated with expansion of protective immune responses such as IFNγ secretion by T_{SCM} cells (Figures 1L–1N).

Furthermore, the impact of SIRT2 inhibition on Wnt/β-catenin signaling and metabolic reprogramming of *M.tb*-specific $CD4^+$ T cells was studied in conjunction by utilizing β-catenin inhibitor, Card, and glycolysis inhibitor, 2DG. A significant reduction in the T_{CM} and T_{SCM} responses was observed in the SIRT2-inhibited samples which were cotreated with either Card or 2DG, indicating that these compounds limit the mechanisms by which AGK2 treatment enhances memory responses (Figure 2). To conclude, the establishment of memory T cells and maintenance was proved to be structured by SIRT2-β-catenin signaling and reprogramming of energy metabolism in response to *M.tb* infections.

To further validate our findings *in vivo*, we repeated BCG vaccination studies along with AGK2 and Card treatment (Figure 7A). Prechallenge lung memory immune landscape of these mice revealed that Card treatment completely abolished the AGK2-induced increase in the T-cell memory responses in BCG-primed animals (Figures 7B–7E). Additional testimony came from the adoptive transfer experiment in $Rag1^{-/-}$ mice where again the T cells isolated from BCG-AGK2-Card vaccinated mice failed to provide protection against *M.tb* infection compared with BCG-AGK2 vaccination (Figure 7F). Moreover, the reduced bacterial burden in mice which derived T cells from BCG-AGK2-vaccinated animals further confirmed the *M.tb*-specific nature of immune responses generated during the BCG-AGK2 vaccination regime (Figure 7G). In continuation, primary infection led to an enhanced bacterial load in the lungs and the spleen of BCG-AGK2-Card vaccinated mice compared with BCG-AGK2 mice, further testifying to the critical role of SIRT2-β-catenin axis in regulating host protective memory responses during *M.tb* infection (Figures 7H and 7I).

To summarize, we report that SIRT2 inhibition by AGK2 plays a critical role in shaping the proteome landscape of $CD4^+$ T cells toward memory phenotype. AGK2 treatment during BCG vaccination augments adaptive memory responses against TB by promoting β-catenin signaling and enhancing the hypermetabolic state of aerobic glycolysis. Being a tractable target, SIRT2 inhibition may be used to strengthen the host defense mechanisms against TB. To sum up, this study opens up a new arena of targeting epigenetic modulators to enhance the efficacy of BCG against pulmonary TB.

Limitations of the study

In this study, we employ mice model of TB to investigate the immunoprophylactic role of AGK2, a well-established SIRT2 inhibitor. To rule out the off-target effects of chemical inhibition, future studies should be performed either with SIRT2 KO mice or a different SIRT2 inhibitor like AK-7. The data should also be validated in human samples.

STAR★METHODS

Detailed methods are provided in the online version of this paper and include the following:

- KEY RESOURCES TABLE
- RESOURCE AVAILABILITY
  - Lead contact
  - Materials availability
  - Data and code availability
- EXPERIMENTAL MODEL AND SUBJECT DETAILS
  - Animals
  - Bacteria
- METHOD DETAILS
  - *M.tb* infection in mice and colony-forming unit (CFU) enumeration
  - Drug administration
  - BCG immunization
  - T cell adoptive transfer
  - Mass spectrometry
  - Reactivation and reinfection experiments

- Flow cytometry: Surface and intracellular staining
- *Ex vivo* splenocytes stimulation and drug treatment
- L-Lactate measurement

- QUANTIFICATION AND STATISTICAL ANALYSIS

SUPPLEMENTAL INFORMATION

Supplemental information can be found online at https://doi.org/10.1016/j.isci.2023.106644.

ACKNOWLEDGMENTS

The mice experiments were conducted in the Department of Biotechnology (DBT)-supported Tuberculosis Aerosol Challenge Facility (TACF) at the International Centre for Genetic Engineering and Biotechnology (ICGEB), New Delhi, India. We acknowledge Ms. Anjna Kumari for her help in cell sorting. I.P. is the recipient of Junior Research Fellowship from the HGK-IYBA grant provided by the DBT, Government of India (GOI). K.N. is the recipient of Junior Research Fellowship from Indian Council of Medical Research, GOI. A.B. is the recipient of the HGK-IYBA Fellowship from Department of Biotechnology, Government of India. We would like to acknowledge the funding support from the Science and Engineering Research Board (SERB), Department of Science and Technology, DBT, GOI, and ICGEB, New Delhi, India. We thank Dr. P. Nagraja, National Institute of Immunology, New Delhi, India for providing Rag1$^{-/-}$ knockout mice.

AUTHOR CONTRIBUTIONS

A.B., I.P., and K.N. performed all the experiments and analyzed the data. A.V. and A.G. performed *ex vivo* experiments. S.C. helped in animal experiments. B.M. and G.T. performed the proteomics experiments. J.S.M. analyzed the proteomics data. A.B., K.N., and V.P.D. wrote the manuscript. A.B. and V.P.D. conceived the hypothesis. A.B. and V.P.D. designed the experiments, analyzed the data, and supervised the experiments.

DECLARATION OF INTERESTS

The authors declare no competing interests.

INCLUSION AND DIVERSITY

While citing references scientifically relevant for this work, we also actively worked to promote gender balance in our reference list. We support inclusive, diverse, and equitable conduct of research.

Received: January 9, 2023
Revised: February 27, 2023
Accepted: April 6, 2023
Published: April 10, 2023

REFERENCES

1. Mayer-Barber, K.D., and Barber, D.L. (2015). Innate and adaptive cellular immune responses to Mycobacterium tuberculosis infection. Cold Spring Harb. Perspect. Med. *5*, a018424. https://doi.org/10.1101/cshperspect.a018424.

2. Korb, V.C., Chuturgoon, A.A., and Moodley, D. (2016). Mycobacterium tuberculosis: manipulator of protective immunity. Int. J. Mol. Sci. *17*, 131. https://doi.org/10.3390/ijms17030131.

3. World Health Organization (2021). Global Tuberculosis Report 2021 (World Health Organization).

4. Fatima, S., Kumari, A., Das, G., and Dwivedi, V.P. (2020). Tuberculosis vaccine: a journey from BCG to present. Life Sci. *252*, 117594. https://doi.org/10.1016/j.lfs.2020.117594.

5. Netea, M.G., Quintin, J., and van der Meer, J.W.M. (2011). Trained immunity: a memory for innate host defense. Cell Host Microbe *9*, 355–361. https://doi.org/10.1016/j.chom.2011.04.006.

6. Kleinnijenhuis, J., Quintin, J., Preijers, F., Joosten, L.A.B., Ifrim, D.C., Saeed, S., Jacobs, C., van Loenhout, J., de Jong, D., Stunnenberg, H.G., et al. (2012). Bacille Calmette-Guérin induces NOD2-dependent nonspecific protection from reinfection via epigenetic reprogramming of monocytes. Proc. Natl. Acad. Sci. USA *109*, 17537–17542. https://doi.org/10.1073/pnas.1202870109.

7. Bali, P., Tousif, S., Das, G., and Van Kaer, L. (2015). Strategies to improve BCG vaccine efficacy. Immunotherapy *7*, 945–948. https://doi.org/10.2217/imt.15.60.

8. Lanzavecchia, A., and Sallusto, F. (2002). Progressive differentiation and selection of the fittest in the immune response. Nat. Rev. Immunol. *2*, 982–987. https://doi.org/10.1038/nri959.

9. Gattinoni, L., Lugli, E., Ji, Y., Pos, Z., Paulos, C.M., Quigley, M.F., Almeida, J.R., Gostick, E., Yu, Z., Carpenito, C., et al. (2011). A human memory T cell subset with stem cell–like properties. Nat. Med. *17*, 1290–1297. https://doi.org/10.1038/nm.2446.

10. Covián, C., Fernández-Fierro, A., Retamal-Díaz, A., Díaz, F.E., Vasquez, A.E., Lay, M.K., Riedel, C.A., González, P.A., Bueno, S.M., and Kalergis, A.M. (2019). BCG-induced cross-protection and development of trained immunity: implication for vaccine design. Front. Immunol. *10*, 2806. https://doi.org/10.3389/fimmu.2019.02806.

11. Schaible, U.E., Linnemann, L., Redinger, N., Patin, E.C., and Dallenga, T. (2017). Strategies to improve vaccine efficacy against tuberculosis by targeting innate immunity. Front. Immunol. *8*, 1755. https://doi.org/10.3389/fimmu.2017.01755.

12. Ellmeier, W., and Seiser, C. (2018). Histone deacetylase function in CD4+ T cells. Nat. Rev. Immunol. *18*, 617–634. https://doi.org/10.1038/s41577-018-0037-z.

13. Wang, J., Hasan, F., Frey, A.C., Li, H.S., Park, J., Pan, K., Haymaker, C., Bernatchez, C., Lee, D.A., Watowich, S.S., and Yee, C. (2020). Histone deacetylase inhibitors and IL21 cooperate to reprogram human effector CD8+ T cells to memory T cells. Cancer Immunol. Res. *8*, 794–805. https://doi.org/10.1158/2326-6066.CIR-19-0619.

14. Hamaidi, I., and Kim, S. (2022). Sirtuins are crucial regulators of T cell metabolism and functions. Exp. Mol. Med. *54*, 207–215. https://doi.org/10.1038/s12276-022-00739-7.

15. North, B.J., and Verdin, E. (2007). Interphase nucleo-cytoplasmic shuttling and localization of SIRT2 during mitosis. PLoS One *2*, e784. https://doi.org/10.1371/journal.pone.0000784.

16. Eskandarian, H.A., Impens, F., Nahori, M.-A., Soubigou, G., Coppée, J.Y., Cossart, P., and Hamon, M.A. (2013). A role for SIRT2-dependent histone H3K18 deacetylation in bacterial infection. Science *341*, 1238858. https://doi.org/10.1126/science.1238858.

17. Bhaskar, A., Kumar, S., Khan, M.Z., Singh, A., Dwivedi, V.P., and Nandicoori, V.K. (2020). Host sirtuin 2 as an immunotherapeutic target against tuberculosis. Elife *9*, e55415. https://doi.org/10.7554/eLife.55415.

18. Gomes, P., Fleming Outeiro, T., and Cavadas, C. (2015). Emerging role of sirtuin 2 in the regulation of mammalian metabolism. Trends Pharmacol. Sci. *36*, 756–768. https://doi.org/10.1016/j.tips.2015.08.001.

19. Hamaidi, I., Zhang, L., Kim, N., Wang, M.-H., Iclozan, C., Fang, B., Liu, M., Koomen, J.M., Berglund, A.E., Yoder, S.J., et al. (2020). Sirt2 inhibition enhances metabolic fitness and effector functions of tumor-reactive T cells. Cell Metabol. *32*, 420–436.e12. https://doi.org/10.1016/j.cmet.2020.07.008.

20. Outeiro, T.F., Kontopoulos, E., Altmann, S.M., Kufareva, I., Strathearn, K.E., Amore, A.M., Volk, C.B., Maxwell, M.M., Rochet, J.-C., McLean, P.J., et al. (2007). Sirtuin 2 inhibitors rescue alpha-synuclein-mediated toxicity in models of Parkinson's disease. Science *317*, 516–519. https://doi.org/10.1126/science.1143780.

21. Nguyen, P., Lee, S., Lorang-Leins, D., Trepel, J., and Smart, D.K. (2014). SIRT2 interacts with β-catenin to inhibit Wnt signaling output in response to radiation-induced stress. Mol. Cancer Res. *12*, 1244–1253. https://doi.org/10.1158/1541-7786.MCR-14-0223-T.

22. O'Sullivan, D. (2019). The metabolic spectrum of memory T cells. Immunol. Cell Biol. *97*, 636–646. https://doi.org/10.1111/imcb.12274.

23. Li, W., and Zhang, L. (2020). Rewiring mitochondrial metabolism for CD8+ T cell memory formation and effective cancer immunotherapy. Front. Immunol. *11*, 1834. https://doi.org/10.3389/fimmu.2020.01834.

24. Tsogtbaatar, E., Landin, C., Minter-Dykhouse, K., and Folmes, C.D.L. (2020). Energy metabolism regulates stem cell pluripotency. Front. Cell Dev. Biol. *8*, 87. https://doi.org/10.3389/fcell.2020.00087.

25. Hong, J.Y., and Lin, H. (2021). Sirtuin modulators in cellular and animal models of human diseases. Front. Pharmacol. *12*, 735044. https://doi.org/10.3389/fphar.2021.735044.

26. Gattinoni, L., Ji, Y., and Restifo, N.P. (2010). Wnt/beta-catenin signaling in T-cell immunity and cancer immunotherapy. Clin. Cancer Res. *16*, 4695–4701. https://doi.org/10.1158/1078-0432.CCR-10-0356.

27. MacDonald, B.T., Tamai, K., and He, X. (2009). Wnt/beta-catenin signaling: components, mechanisms, and diseases. Dev. Cell *17*, 9–26. https://doi.org/10.1016/j.devcel.2009.06.016.

28. Devotta, A., Hong, C.-S., and Saint-Jeannet, J.-P. (2018). Dkk2 promotes neural crest specification by activating Wnt/β-catenin signaling in a GSK3β independent manner. Elife *7*, e34404. https://doi.org/10.7554/eLife.34404.

29. Schepsky, A., Bruser, K., Gunnarsson, G.J., Goodall, J., Hallsson, J.H., Goding, C.R., Steingrimsson, E., and Hecht, A. (2006). The microphthalmia-associated transcription factor Mitf interacts with beta-catenin to determine target gene expression. Mol. Cell Biol. *26*, 8914–8927. https://doi.org/10.1128/MCB.02299-05.

30. Yin, C., Zhang, Y., Hu, L., Tian, Y., Chen, Z., Li, D., Zhao, F., Su, P., Ma, X., Zhang, G., et al. (2018). Mechanical unloading reduces microtubule actin crosslinking factor 1 expression to inhibit β-catenin signaling and osteoblast proliferation. J. Cell. Physiol. *233*, 5405–5419. https://doi.org/10.1002/jcp.26374.

31. Mattes, B., Dang, Y., Greicius, G., Kaufmann, L.T., Prunsche, B., Rosenbauer, J., Stegmaier, J., Mikut, R., Özbek, S., Nienhaus, G.U., et al. (2018). Wnt/PCP controls spreading of Wnt/β-catenin signals by cytonemes in vertebrates. Elife *7*, e36953. https://doi.org/10.7554/eLife.36953.

32. Gattinoni, L., Zhong, X.-S., Palmer, D.C., Ji, Y., Hinrichs, C.S., Yu, Z., Wrzesinski, C., Boni, A., Cassard, L., Garvin, L.M., et al. (2009). Wnt signaling arrests effector T cell differentiation and generates CD8+ memory stem cells. Nat. Med. *15*, 808–813. https://doi.org/10.1038/nm.1982.

33. Sarikhani, M., Mishra, S., Maity, S., Kotyada, C., Wolfgeher, D., Gupta, M.P., Singh, M., and Sundaresan, N.R. (2018). SIRT2 deacetylase regulates the activity of GSK3 isoforms independent of inhibitory phosphorylation. Elife *7*, e32952. https://doi.org/10.7554/eLife.32952.

34. Tan, S.Y., Kelkar, Y., Hadjipanayis, A., Shipstone, A., Wynn, T.A., and Hall, J.P. (2020). Metformin and 2-deoxyglucose collaboratively suppress human CD4+ T cell effector functions and activation-induced metabolic reprogramming. J. Immunol. *205*, 957–967. https://doi.org/10.4049/jimmunol.2000137.

35. Gattinoni, L., Speiser, D.E., Lichterfeld, M., and Bonini, C. (2017). T memory stem cells in health and disease. Nat. Med. *23*, 18–27. https://doi.org/10.1038/nm.4241.

36. Bhatt, D., and Ghosh, S. (2014). Regulation of the NF-κB-Mediated transcription of inflammatory genes. Front. Immunol. *5*, 71. https://doi.org/10.3389/fimmu.2014.00071.

37. Park, S., Gwak, J., Han, S.J., and Oh, S. (2013). Cardamonin suppresses the proliferation of colon cancer cells by promoting β-catenin degradation. Biol. Pharm. Bull. *36*, 1040–1044. https://doi.org/10.1248/bpb.b13-00158.

38. Pelicano, H., Martin, D.S., Xu, R.-H., and Huang, P. (2006). Glycolysis inhibition for anticancer treatment. Oncogene *25*, 4633–4646. https://doi.org/10.1038/sj.onc.1209597.

39. Andersen, P., and Doherty, T.M. (2005). The success and failure of BCG — implications for a novel tuberculosis vaccine. Nat. Rev. Microbiol. *3*, 656–662. https://doi.org/10.1038/nrmicro1211.

40. Pai, M., Behr, M.A., Dowdy, D., Dheda, K., Divangahi, M., Boehme, C.C., Ginsberg, A., Swaminathan, S., Spigelman, M., Getahun, H., et al. (2016). Nat. Rev. Dis. Prim. *2*, 16076. https://doi.org/10.1038/nrdp.2016.76.

41. Flynn, J.L., and Chan, J. (2001). Immunology of tuberculosis. Annu. Rev. Immunol. *19*, 93–129. https://doi.org/10.1146/annurev.immunol.19.1.93.

42. Van Gool, S.W., Vandenberghe, P., de Boer, M., and Ceuppens, J.L. (1996). CD80, CD86 and CD40 provide accessory signals in a multiple-step T-cell activation model. Immunol. Rev. *153*, 47–83. https://doi.org/10.1111/j.1600-065x.1996.tb00920.x.

43. Sakai, S., Mayer-Barber, K.D., and Barber, D.L. (2014). Defining features of protective CD4 T cell responses to Mycobacterium tuberculosis. Curr. Opin. Immunol. *29*, 137–142. https://doi.org/10.1016/j.coi.2014.06.003.

44. Sud, D., Bigbee, C., Flynn, J.L., and Kirschner, D.E. (2006). Contribution of CD8 $^{+}$ T cells to control of *Mycobacterium tuberculosis* infection. J. Immunol. *176*, 4296–4314. https://doi.org/10.4049/jimmunol.176.7.4296.

45. Smith, S.G., Zelmer, A., Blitz, R., Fletcher, H.A., and Dockrell, H.M. (2016). Polyfunctional CD4 T-cells correlate with in vitro mycobacterial growth inhibition following Mycobacterium bovis BCG-vaccination of infants. Vaccine *34*, 5298–5305. https://doi.org/10.1016/j.vaccine.2016.09.002.

46. Nandakumar, S., Kannanganat, S., Posey, J.E., Amara, R.R., and Sable, S.B. (2014). Attrition of T-cell functions and simultaneous upregulation of inhibitory markers correspond with the waning of BCG-induced protection against tuberculosis in mice. PLoS One *9*, e113951. https://doi.org/10.1371/journal.pone.0113951.

47. Mpande, C.A.M., Dintwe, O.B., Musvosvi, M., Mabwe, S., Bilek, N., Hatherill, M., Nemes, E., and Scriba, T.J.; SATVI Clinical Immunology Team (2018). Functional, antigen-specific stem cell memory (TSCM) CD4+ T cells are induced by human Mycobacterium tuberculosis infection. Front. Immunol. *9*, 324. https://doi.org/10.3389/fimmu.2018.00324.

48. Lange, J., Rivera-Ballesteros, O., and Buggert, M. (2022). Human mucosal tissue-resident memory T cells in health and disease. Mucosal Immunol. *15*, 389–397. https://doi.org/10.1038/s41385-021-00467-7.

49. Bhattacharya, D., Dwivedi, V.P., Kumar, S., Reddy, M.C., Van Kaer, L., Moodley, P., and Das, G. (2014). Simultaneous inhibition of T helper 2 and T regulatory cell differentiation by small molecules enhances Bacillus Calmette-Guerin vaccine efficacy against tuberculosis. J. Biol. Chem. *289*, 33404–33411. https://doi.org/10.1074/jbc.M114.600452.

50. Kim, H.-S., Vassilopoulos, A., Wang, R.-H., Lahusen, T., Xiao, Z., Xu, X., Li, C., Veenstra, T.D., Li, B., Yu, H., et al. (2011). SIRT2 maintains genome integrity and suppresses tumorigenesis through regulating APC/C activity. Cancer Cell *20*, 487–499. https://doi.org/10.1016/j.ccr.2011.09.004.

51. Lewinsohn, D.A., Lewinsohn, D.M., and Scriba, T.J. (2017). Polyfunctional CD4+ T cells as targets for tuberculosis vaccination. Front. Immunol. *8*, 1262. https://doi.org/10.3389/fimmu.2017.01262.

52. Kared, H., Tan, S.W., Lau, M.C., Chevrier, M., Tan, C., How, W., Wong, G., Strickland, M., Malleret, B., Amoah, A., et al. (2020). Immunological history governs human stem cell memory CD4 heterogeneity via the Wnt signaling pathway. Nat. Commun. *11*, 821. https://doi.org/10.1038/s41467-020-14442-6.

53. Jasenosky, L.D., Scriba, T.J., Hanekom, W.A., and Goldfeld, A.E. (2015). T cells and adaptive immunity to Mycobacterium tuberculosis in humans. Immunol. Rev. *264*, 74–87. https://doi.org/10.1111/imr.12274.

54. Villarino, A.V., Kanno, Y., Ferdinand, J.R., and O'Shea, J.J. (2015). Mechanisms of Jak/STAT signaling in immunity and disease. J. Immunol. *194*, 21–27. https://doi.org/10.4049/jimmunol.1401867.

55. Chang, H.-C., and Guarente, L. (2014). SIRT1 and other sirtuins in metabolism. Trends Endocrinol. Metabol. *25*, 138–145. https://doi.org/10.1016/j.tem.2013.12.001.

56. Jeng, M.Y., Hull, P.A., Fei, M., Kwon, H.-S., Tsou, C.-L., Kasler, H., Ng, C.-P., Gordon, D.E., Johnson, J., Krogan, N., et al. (2018). Metabolic reprogramming of human CD8+ memory T cells through loss of SIRT1. J. Exp. Med. *215*, 51–62. https://doi.org/10.1084/jem.20161066.

57. Ping, C.P., Tengku Mohamad, T.A.S., Akhtar, M.N., Perimal, E.K., Akira, A., Israf Ali, D.A., and Sulaiman, M.R. (2018). Antinociceptive effects of cardamonin in mice: possible involvement of TRPV$_1$, glutamate, and opioid receptors. Molecules *23*, 2237. https://doi.org/10.3390/molecules23092237.

58. Tripathi, G., Sharma, N., Bindal, V., Yadav, M., Mathew, B., Sharma, S., Gupta, E., Singh Maras, J., and Sarin, S.K. (2022). Protocol for global proteome, virome, and metaproteome profiling of respiratory specimen (VTM) in COVID-19 patient by LC-MS/MS-based analysis. STAR Protoc. *3*, 101045. https://doi.org/10.1016/j.xpro.2021.101045.

59. Zhou, Y., Zhou, B., Pache, L., Chang, M., Khodabakhshi, A.H., Tanaseichuk, O., Benner, C., and Chanda, S.K. (2019). Metascape provides a biologist-oriented resource for the analysis of systems-level datasets. Nat. Commun. *10*, 1523. https://doi.org/10.1038/s41467-019-09234-6.

60. Malehmir, M., Pfister, D., Gallage, S., Szydlowska, M., Inverso, D., Kotsiliti, E., Leone, V., Peiseler, M., Surewaard, B.G.J., Rath, D., et al. (2019). Platelet GPIbα is a mediator and potential interventional target for NASH and subsequent liver cancer. Nat. Med. *25*, 641–655. https://doi.org/10.1038/s41591-019-0379-5.

STAR★METHODS

KEY RESOURCES TABLE

REAGENT or RESOURCE	SOURCE	IDENTIFIER
Antibodies		
CD3-BV421	Biolegend	Cat# 100227; RRID: AB_10900227
CD4-PerCPCy5.5	Biolegend	Cat# 100434; RRID:AB_893324
CD8-APCCy7	Biolegend	Cat# 100714; RRID:AB_312753
CD44-PE	Biolegend	Cat# 103024; RRID:AB_493687
CD44-FITC	Biolegend	Cat# 163605; RRID:AB_2894435
CD62L-APC	Biolegend	Cat# 104412; RRID:AB_313099
CD69-PE	Biolegend	Cat# 104508; RRID:AB_313111
Sca1-PeCy5	Biolegend	Cat# 108109; RRID:AB_313346
CD122-PeCy7	Biolegend	Cat# 123215; RRID:AB_2562894
CD103-PeCy7	Biolegend	Cat# 121425; RRID:AB_2563690
IFNγ-BV510	Biolegend	Cat# 505841; RRID:AB_2562187
IFNγ-PerCPCy5.5	Biolegend	Cat# 505821; RRID:AB_961361
IL17-BV650	Biolegend	Cat# 506929; RRID:AB_11126980
IL17-APCCy7	Biolegend	Cat# 506939; RRID:AB_2565780
CD11b-APCCy7	Biolegend	Cat# 101226; RRID:AB_830642
CD11c-APC	Biolegend	Cat# 117309; RRID:AB_313778
CD40-PE	Biolegend	Cat# 157506; RRID:AB_2860731
CD80-FITC	Biolegend	Cat# 104705; RRID:AB_313126
CD86-PerCPCy5.5	Biolegend	Cat# 105027; RRID:AB_893420
TNFα-PE	Biolegend	Cat# 506305; RRID:AB_315426
IL2-FITC	Biolegend	Cat# 503805; RRID:AB_315299
CD3-FITC	Biolegend	Cat# 100204; RRID:AB_312661
CD3-BV510	Biolegend	Cat# 100233; RRID:AB_2561387
CD3-BV650	Biolegend	Cat# 100229; RRID:AB_11204249
CD3-APC	Biolegend	Cat# 100235; RRID:AB_2561455
CD3-PE	Biolegend	Cat# 100205; RRID:AB_312662
CD3-PeCy5	Biolegend	Cat# 100273; RRID:AB_2894410
CD3-PeCy7	Biolegend	Cat# 100219; RRID:AB_1732068
Ac-β-catenin	CST	Cat# 9030; RRID:AB_2797689
Acetyl-H3	Abcam	Cat# ab47915; RRID:AB_873860
Acetyl-NFκB-p65	Abcam	Cat# ab19870; RRID:AB_776753
SIRT2	Abcam	Cat# ab211033; RRID:AB_2927614
Chemicals		
AGK2	Merck	A8231-25MG
Cardamonin	Merck	C8249-5MG
2-Deoxy-D-Glucose	Merck	D8375

RESOURCE AVAILABILITY

Lead contact

Further information and requests for resources and reagents should be directed to and will be fulfilled by the lead contact, Ashima Bhaskar (ashimabhaskar@gmail.com).

Materials availability

This study did not generate new unique reagents.

Data and code availability

- Proteomics data reported in this paper will be shared by the lead contact upon request.
- This paper does not report original code.
- Any additional information required to reanalyze the data reported in this paper is available from the lead contact upon request.

EXPERIMENTAL MODEL AND SUBJECT DETAILS

Animals

Experimentation on animals was implemented according to the rules and regulations approved by the Institutional Animals Ethics Committee at the International Centre for Genetic Engineering and Biotechnology (ICGEB) New Delhi, India, along with guidelines of the Department of Biotechnology (DBT), Government of India. Mice used for experiments were sacrificed ethically by asphyxiation with carbon dioxide in compliance with institutional and DBT guidelines. C57BL/6 and Rag1$^{-/-}$ mice (female, 6–8 weeks of age) were maintained and acquired from the animal facility of ICGEB, New Delhi, India for the experiments.

Bacteria

M.tb laboratory strain H37Rv and *M.bovis* strain BCG were used in this study. GFP expressing mycobacteria was generated in the H37Rv background. For infections, the aliquots of cryopreserved cultures in 20% glycerol were revived from -80°C and grown till the mid-log phase in Middlebrook 7H9 (Difco) medium supplemented with 0.2% glycerol (Sigma), 0.05% Tween-80 (Sigma) and 10% ADC (albumin, dextrose, and catalase; Difco).

METHOD DETAILS

M.tb infection in mice and colony-forming unit (CFU) enumeration

Mice were infected with *M.tb* H37Rv through an aerosol route employing Madison Aerosol Chamber (University of Wisconsin, Madison, WI) with the nebulizer standardized to deliver ~110 bacilli to the lungs of each mouse. Cryopreserved mycobacterial stocks were retrieved from -80°C freezer and 15ml of *M.tb* H37Rv single-cell suspension was prepared for infection. Post-infection, on day 1, 3 mice were randomly euthanized and the lungs were homogenized using 0.2 mm filtered PBS. Neat and diluted homogenates were plated onto Middlebrook 7H11(Difco, USA) plates supplemented with 10% OADC (Difco, USA) and were incubated at 37°C for 21–28 days. Mice from distinct groups were sacrificed at indicated time periods and the CFU was performed from the lungs and the spleen homogenates.

Drug administration

For *in vivo* experiments, 5 mg/kg of AGK2, Abcam (SIRT-2 inhibitor) and 2.5 mg/kg of Card (Sigma) was administered intraperitoneally to mice thrice a week for 2 weeks, whereas control mice were given vehicle only. The inhibitor doses were decided based on the previous literature.[17,57]

BCG immunization

Mice were immunized subcutaneously 1 × 10^6 CFU BCG prepared in 100 µl of sterile saline. 7 days post-vaccination, mice were treated with AGK2 and or Card intraperitoneally. Subsequent to the treatment, mice were rested for 30 days and then challenged with *M.tb* strain H37Rv by the aerosol route. Lungs and spleen were harvested to determine the bacterial load and for evaluation of immune responses at different days post-infection.

T cell adoptive transfer

Spleen from mice of different groups (a) Naive, (b) BCG immunized, (c) BCG-AGK2 co-immunized, (d) BCG-AGK2-CARD co-immunized was isolated and macerated by sterile frosted glass slides to form single cell suspension. The cells were stained with antibodies against CD3 and CD4 followed by sorting of $CD3^+CD4^+$ T cells using FACS Aria (BD Biosciences) and overnight cultured in complete RPMI media. One million cells were intravenously administered to Rag1$^{-/-}$ mouse and 5 days post transfer, the recipient

mice were challenged with a low dose of GFP expressing *M.tb* through aerosol and bacterial burden was assessed 25 days post-infection.

Mass spectrometry

Control and AGK2 treated $CD4^+$ T cells were subjected to protein extraction and 10 μg of equivalent proteins were subjected to reduction, alkylation and digestion for 24 hrs at 37°C using Trypsin Gold, Mass Spectrometry Grade (Promega Corporation, WA, USA). Post-desalting, the samples containing purified peptides were subjected to LC-MS/MS analysis. On a 25-cm analytical C18 column (C18, 3 μm, 100 Å), these peptides were eluted using (5–95%) gradient of buffer B (aqueous 80% acetonitrile and 0.1% formic acid) at a flow rate of 300 nL/min for 2.5 hrs. Post elution these peptides were subjected to nano-electrospray ionisation and Tandem mass spectrometry (MS/MS) using Q-ExactiveTM Plus (Thermo Fisher Scientific, San Jose, CA, United States) at the collision-induced dissociation mode with the electrospray voltage was 2.3 kV. Further data was analysed using Proteome Discoverer (version 2.0, Thermo Fisher Scientific, Waltham, MA, United States). Uniprot *Mus musculus* (Mouse) database (UP000000589) with Mascot algorithm (Mascot 2.4, Matrix Science) was used.[58] Identified proteins were subjected to standard statistical analysis, network and pathway analysis.[59,60]

Reactivation and reinfection experiments

Vulnerability to infection was evaluated by reinfection and reactivation studies. Mice infected with low dose aerosol of *M.tb* strain H37Rv were treated with INH (100 mg/L) and RIF (40 mg/kg) in drinking water for 12 weeks. The mice were further rested for the next 30 days. To evaluate the reactivation rate, mice were administered with dexamethasone (5 mg/kg) intraperitoneally, three times per week for 30 days followed by CFU determination and host protective immune response. The reinfection group was again challenged with *M.tb* and sacrificed post 30 days to enumerate CFU and analyse the immunological profiles.

Flow cytometry: Surface and intracellular staining

Lungs and spleen isolated from individual groups of mice were macerated with frosted slides in ice-cold RPMI 1640 (Invitrogen) supplemented with 10% FBS to prepare single-cell suspension. RBC lysis buffer was used to lyse RBCs and then cells were washed with RPMI 1640 supplemented with 10 % FBS. The cells were seeded at the density of $1x\ 10^6$ cells per ml. The cells were stimulated overnight with 10 μg/ml of H37Rv-derived complete soluble antigen (CSA). Prior to the surface and intracellular staining, the cell viability was determined by 7-Aminoactinomycin D (7AAD) and only if it was more than 95%, the cells were processed further. For intracellular cytokine staining, the cells were treated with 0.5 μg/ml Brefeldin A and 0.5 μg/ml Monensin (BioLegend) for 4 hrs. Cells were washed doubly with FACS buffer (1XPBS and 3% FBS) and stained with antibodies specific to the surface markers in the dilutions as suggested by the manufacturer (1:100). Post staining, cells were fixed with 100 μl fixation buffer (BioLegend) for 30 min. 1X permeabilization buffer (BioLegend) was used to permeabilize the cells for staining the intracellular cytokines or other proteins. Secondary antibody attached with Alexa Fluor 488 was used against non-fluorochrome tagged antibodies. Isotype controls and fluorescence minus one (FMO) controls were used in each experiment for gating. The samples were analysed by BD LSRFortessa^{TM} Cell Analyzer – Flow Cytometer (BD Biosciences) and data analysis was performed by FlowJo (Tree star, USA).

Ex vivo splenocytes stimulation and drug treatment

Spleens from BCG vaccinated and *M.tb* infected mice were isolated and macerated using autoclaved frosted slides in sterile PBS. CSA-stimulated splenocytes were treated with 10 μM AGK2, 2.5 μM Cardamonin (Card), and 200 mM 2-Deoxy-D-glucose (2DG) for 48 h followed by immune profiling.

L-Lactate measurement

To determine the extracellular L-Lactate levels, the culture supernatants of sorted $CD4^+$ T cells treated with AGK2 and 2DG were collected and the L-Lactate assay was performed using the L- Lactate assay kit (Cayman Chemicals) as per the manufacturer's protocol.

QUANTIFICATION AND STATISTICAL ANALYSIS

Every animal experiment was performed once with five mice per group per time point (n = 5). Significant differences between the group mean were determined by one-way ANOVA or t-test. $p<0.05$ was considered significant.